Reviewed Preprint
v1 • November 13, 2025
Not revised

Reviewed Preprint
v2 • April 2, 2026
Revised by authors

For correspondence:
fwhuang2@stanford.edu

Competing interests: No competing interests declared

Reviewing editor: Helen Scharfman, Nathan Kline Institute, United States

Excitatory cholecystokinin neurons in CA3 area regulate the navigation learning and neuroplasticity

Fengwen Huang[1,2], **Abdul Baset**[2], **Stephen Temitayo Bello**[2]

[1]Department of Neuroscience, City University of Hong Kong, Hong Kong, China • [2]Department of Ophthalmology, Stanford University School of Medicine, Palo Alto, United States

eLife Assessment

This study presents data suggesting that excitatory cholecystokinin (CCK)-expressing neurons in hippocampal area CA3 influence hippocampal-dependent memory using multiple methods to manipulate excitatory CCK-expressing CA3 neurons. The study is **valuable**, particularly considering that most past studies of CCK-expressing neurons have focused on those neurons that co-express CCK and GABA. Currently, the strength of evidence is **incomplete**, but it would improve if evidence of specificity was provided and other concerns were addressed. If this is not possible, the conclusions, particularly those requiring evidence of specific targeting of excitatory neurons, should be modified accordingly.

https://doi.org/10.7554/eLife.109001.2.sa4

Abstract

Hippocampus, a key hub of neural circuits for spatial learning and memory, has attracted tremendous studies. Neuronal information processing in the hippocampus can be regulated by many types of neuropeptides. Cholecystokinin (CCK), the most abundant neuropeptide in the central nervous system which is involved in modulating neuronal functions, such as cognition, memory and neuroplasticity, is widely expressed in the hippocampus. However, whether local excitatory CCK neurons modulates hippocampal function is still unclear. In this study, we showed that CA1 pyramidal neurons receive projections from excitatory CCK neurons in area CA3 ($CA3^{CCK}$ neurons). Subsequently, activation of the CA1-projecting $CA3^{CCK}$ neurons triggers the release of CCK. Then, we found that activity of $CA3^{CCK}$-CA1 neurons supports the hippocampal-dependent tasks. Furthermore, inhibition of $CA3^{CCK}$-CA1 projections or knockdown of $CA3^{CCK}$ gene expression markedly impaired the behavioral tasks and neuroplasticity. Taken together, these results may add to a better understanding of how neuromodulators regulate the neural functions in central nervous system.

Introduction

Neuropeptides are expressed and secreted throughout the mammalian brain where they play key roles in modulating neuronal activities and behaviors (Swaab 1982; Merighi et al., 2011; De Wied 1997). Long-term potentiation (LTP) and long-term depression (LTD) have been considered cellular mechanisms correlated with learning and memory in the central nervous system (CNS) (Grasselli and Hansel 2014). Hippocampus is a unique brain region that is critically involved in learning and memory (Ranganath and Hsieh 2016), and how neuromodulations affect the function of the hippocampal system has attracted lots of interest (Gedankien et al., 2023; Broussard et al., 2016; Li and Gao 2016; Karayol et al., 2021).

During the past decades, many studies have identified the neuronal mechanisms that guide neuropeptides across the hippocampal function and examined whether neuropeptides undergo specific adaptations in response to external innervation. However, most investigations focus on the classical monoamine neuromodulators, including acetylcholine (Ach), dopamine (DP), norepinephrine (NE), serotonin (ST), etc (Gedankien et al., 2023; Broussard et al., 2016; Li and Gao 2016; Karayol et al., 2021). Ach can regulate neuronal excitability and synaptic transmission in the mammalian brain (Takács et al., 2018). Several studies have demonstrated that stress increases Ach release in a brain region-specific manner (Picciotto et al., 2012; Mineur et al., 2013). For example, stress-induced increase in Ach level in the rat hippocampus and cortical area. DP is a critical modulator in neuronal circuitry, which has been shown to be involved in a variety of behavioral phenomena in the hippocampus, such as episodic memory formation (Chowdhury et al., 2012), spatial learning (Kempadoo et al., 2016), and synaptic plasticity (Hamilton et al., 2010). DP innervation from the midbrain is mainly via the dopamine receptor (D1/D5) when it is released into the dorsal hippocampus (Cai and Ford 2018). Additionally, the role of NE in memory retrieval requires signaling through the β1-adrenergic receptor in the hippocampus (Chang et al., 2011). The hippocampus has one of the denser inputs of adrenergic terminals (containing NE) in the CNS, indicating that the adrenergic system plays a role in learning and memory (Goodman et al., 2021). Interestingly, high concentration of serotoninergic fibers in the forebrain is in stratum lacunosum-moleculare (SLM) of hippocampal areas CA1 and CA3, where the axons of layer III neurons in the entorhinal cortex form excitatory synapses with the distal apical dendrites of pyramidal cells (Cai et al., 2013). This temporoammonic pathway is required for some spatial recognition tasks and for long-term consolidation of spatial memory. All these studies implied that neuropeptides play a critical role in the hippocampal system and influence subsequent behaviors.

Cholecystokinin (CCK), one of the most abundant neuropeptides in the CNS (Ma and Giardino 2022), has not received much attention and its function in the hippocampal system has been generally underestimated. Although several reports have shown that CCK enhances the excitatory synaptic transmission in the hippocampus and improves learning performance (Wei et al., 2013; Reisi et al., 2015). However, the exact mechanism by which CCK regulates the hippocampus plasticity and hippocampus-dependent behaviors has not yet been fully elucidated. To address this knowledge gap, we adopted the transgenic mice, optogenetics, GPCR-based sensor, extracellular recording, chemogenetics, RNA interference technique, calcium recording and behavioral task to investigate: 1) the distribution profile of CCK-positive neurons in the CA3 area of dorsal hippocampus (DHP), 2) activation of $CA3^{CCK}$ neurons secrets the CCK at hippocampal SC-CA1 synapses. 3) the causal relationship between the Ca^{2+} response of excitatory $CA3^{CCK}$ neurons and hippocampal functions. This study should bring conceptual advances to the foundation of neuropeptide modulation and the studies of hippocampus-dependent learning and memory.

Results

Distribution profile of CCK-positive neurons in the DHP

Although many studies have well documented the role of inhibitory CCK in the hippocampus (Klausberger et al., 2005; Ali 2007; Hefft and Jonas 2005), the function of excitatory CCK in the hippocampus is still unclear. To address this issue, we developed the transgenic CCK Cre::Ai14 (Tdtomato) reporter mice that express the red fluorescent protein tdTomato upon Cre-mediated recombination. This mouse line is suited in examining the distribution profile of CCK positive neurons in the dorsal hippocampus (DHP) (Figure 1A-B). Interestingly, we found that the proportion of CCK positive neurons in area CA1 and CA3 of CCK Cre/Ai14 mice was around 8.50 % and 20.34 %, respectively (Figure 1C-D). We further examined the properties of these CCK neurons in areas CA3, which may send dense CCK^{+} projections to the area CA1. Interestingly, excitatory neuronal marker CamkIIα was intensively colocalized with Tdtomato expressing CCK neurons in the area CA3 (Figure 1E). Moreover. the CCK proteins also show high co-localization in excitatory neurons in CA3 area (Figure 1F).

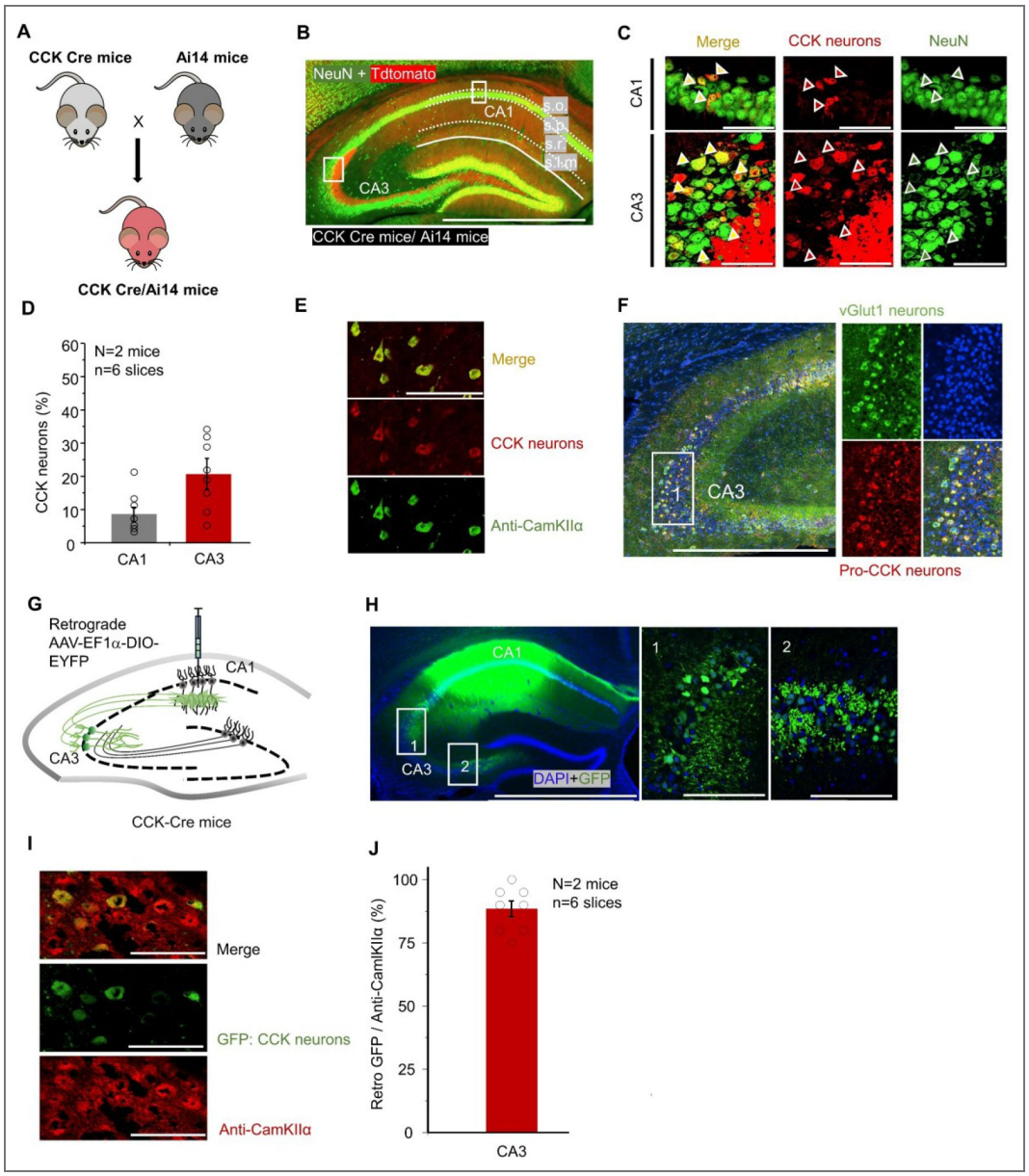

Figure 1. The distribution profile of CCK-positive neurons in the dorsal hippocampus.

(A) Schematic illustrating the breeding strategy used to generate CCK-Cre/Ai14 reporter mice, in which CCK-expressing neurons are labeled with tdTomato. **(B)** Representative fluorescence image of a dorsal hippocampal slice from a CCK-Cre/Ai14 mouse immunostained with the pan-neuronal marker NeuN (rabbit anti-NeuN, Alexa Fluor 488), showing overall hippocampal anatomy. Scale bar, 1000 μm. **(C)** Higher-magnification images showing CCK-positive neurons identified by tdTomato expression (red) colocalized with NeuN immunofluorescence (green) in hippocampal CA1 and CA3 regions. Scale bar, 50 μm. **(D)** Quantification of the number of CCK-positive neurons in the CA1 and CA3 regions of the dorsal hippocampus. **(E)** Representative image of co-immunofluorescent labeling of CCK-positive neurons with the excitatory neuronal marker CaMKIIα in the CA3 region. Scale bar, 100 μm. **(F)** Fluorescence image showing colocalization of endogenous CCK protein (Pro-CCK) with an excitatory neuronal marker in the CA3 region. Scale bar, 1000 μm. **(G)** Schematic diagram illustrating the viral injection strategy. A Cre-dependent AAV (AAV-EF1α-DIO-EYFP; 6.5×10^{12} vg/mL, 50 nL) was injected into the CA1 region of CCK-Cre mice to label CCK-expressing neurons and their projections. **(H)** Representative fluorescence images showing AAV expression in the hippocampal CA1 region (left) and retrogradely labeled neurons in the CA3 region (right). Scale bars: 1000 μm (left), 100 μm (right). **(I)** Representative image showing colocalization of retrogradely labeled GFP-positive neurons with the excitatory neuronal marker CaMKIIα (rabbit anti-CaMKIIα, red) in the CA3 region. Scale bar, 100 μm. **(J)** Co-immunofluorescent staining demonstrating colocalization of GFP with CaMKIIα in CA3 neurons of CCK-Cre mice, confirming the excitatory identity of retrogradely labeled CCK-expressing neurons. *$p < 0.05$, **$p < 0.01$, ***$p < 0.001$; ns not significant. Data are reported as mean ± SEM.

Furthermore, to validate the projection of CA1-projecting $CA3^{CCK}$ neurons in the DHP, we injected the Cre-dependent retrograde axonal transport of AAV (Retro-AAV-EF1α-DIO-EYFP) into the area CA1 (Figure 1G). Unsurprisingly, CA3 neurons were widely labelled with green fluorescent protein (GFP; Figure 1H). Moreover, high degree of colocalization between CamKIIα marker and GFP was observed in the area CA3 (Figure 1I-J; 90.15± 15 %). These anatomy results suggest that excitatory CA3 neurons are densely expressed and may exerts neuronal functions in central nervous system.

Excitatory CA3 neurons can secret the neuropeptide CCK

Next, to investigate the neurotransmission property of the excitatory CCK neurons in CA3 area ($CA3^{CCK}$), we utilized the Cre-dependent excitatory AAV (AAV9-DIO-CamKIIα-ChrimsonR-mCherry) to specifically target the excitatory $CA3^{CCK}$ neurons in CCK-Cre mice (Figure 2A). The AAV shows high specificity for targeting the CCK positive neurons in the CA3 area (93.50 ± 1.97%; sFigure 1). Four weeks after the AAV injection and expression in *vivo*, robust expression of ChrimsonR-mCherry was observed in $CA3^{CCK}$ neurons (Figure 2B-C). Subsequently, we used the 636 nm wavelength light to activate and elicit the field excitatory post synaptic potentials (L-fEPSPs) in ChrimsonR-mCherry expressing brain section (Figure 2D). Intriguingly, we noticed that the L-fEPSPs were almost completely blocked by the AMPA receptor antagonist (CNQX; 20 μM) and NMDA receptor antagonist (APV; 100 μM) in the area CA1, suggesting an excitatory nature of CA1-projecting $CA3^{CCK}$ pathway (Figure 2E-F).

Based on our recent work, CCK signaling in the hippocampus is predominantly mediated by CCK-B receptors, which play a critical role in regulating synaptic plasticity and spatial memory-related behaviors. To determine whether the neuropeptide CCK can be secreted from the CA3 derived excitatory CA3-CA1 projections, we adopted the GPCR-based CCK-BR sensor to monitor the release of CCK from the CA3-CA1 terminals in CA1 area under the external light stimulation (Figure 2G). To achieve this goal, AAV9-DIO-CamKIα-ChrimsonR-mCherry and AAV9-hSyn-CCK-GFP-2.3 (AAV9-hSyn-GFP as control) were injected into the CA3 and CA1 area to target the CA3-CA1 projection and CA1 pyramidal neurons (CA1 PNs) in CCK-Cre mice (Figure 2H). Subsequently, stimulation fiber and recording fiber were implanted upon the CA3 and CA1 area. Four weeks after the AAVs injection and expression (Figure 2I-J), high-frequency theta burst light stimulation (L-TBS) was delivered to the simulation fiber (Figure 2K), which mimic the neural rhythm in hippocampus in *vivo*. Interestingly, transient increase in CCK sensor was monitored by L-TBS of ChrimsonR-expressing $CA3^{CCK}$ neurons, while no significant amplification was found in control (Figure 2L-N; Two samples T-Test, t = 3.79 df = 10, p = 0.004). These results indicates that neuropeptide CCK can be secreted from the excitatory $CA3^{CCK}$ neurons under the mimic physiological conditions.

$CA3^{CCK}$ neurons fire actively during hippocampal-dependent tasks

We next wonder about the activity status of $CA3^{CCK}$ neurons during hippocampal-dependent tasks (Figure 3A). Thus, we injected the AAV9-CamkIIα-DIO-GCaMP6s into the area CA3 of CCK Cre mice to monitor the calcium-response of $CA3^{CCK}$ neurons during the behavioral task (Figure 3B). The AAV displays high specificity for infecting the CCK positive neurons in the CA3 area (93.00 ± 1.33 %; sFigure 2). In novel object location (NOL) task, mice spent comparable time on object exploration between object 1 (O1) and object 2 (O2) in the training phase, while mice spent significantly more time on interacting with object in the novel place (O2") compared with the object in the familiar site (Figure 3C; two way mixed ANOVA, Bonferroni adjustment; $F_{1,10}$ = 4.58, p = 0.05; Training: O1 11.42 ± 1.56 s v.s. O2 10.62 ± 2.18 s, p = 0.73; Testing: O1 8.62 ± 0.99 s v.s. O2": 13.95 ± 1.60 s, p = 0.02). Concurrently, we examined the Ca^{2+} responses of excitatory $CA3^{CCK}$ neurons during object exploration. Interestingly, we observed that object exploration elicited a significant increase in fluorescence intensity in both training phase and testing phase (Figure 3D-E). Moreover, Ca^{2+}signal of $CA3^{CCK}$ neurons elicited by novel locations also show significant difference compared with familiar locations (Figure 3F; two way mixed ANOVA, Bonferrori

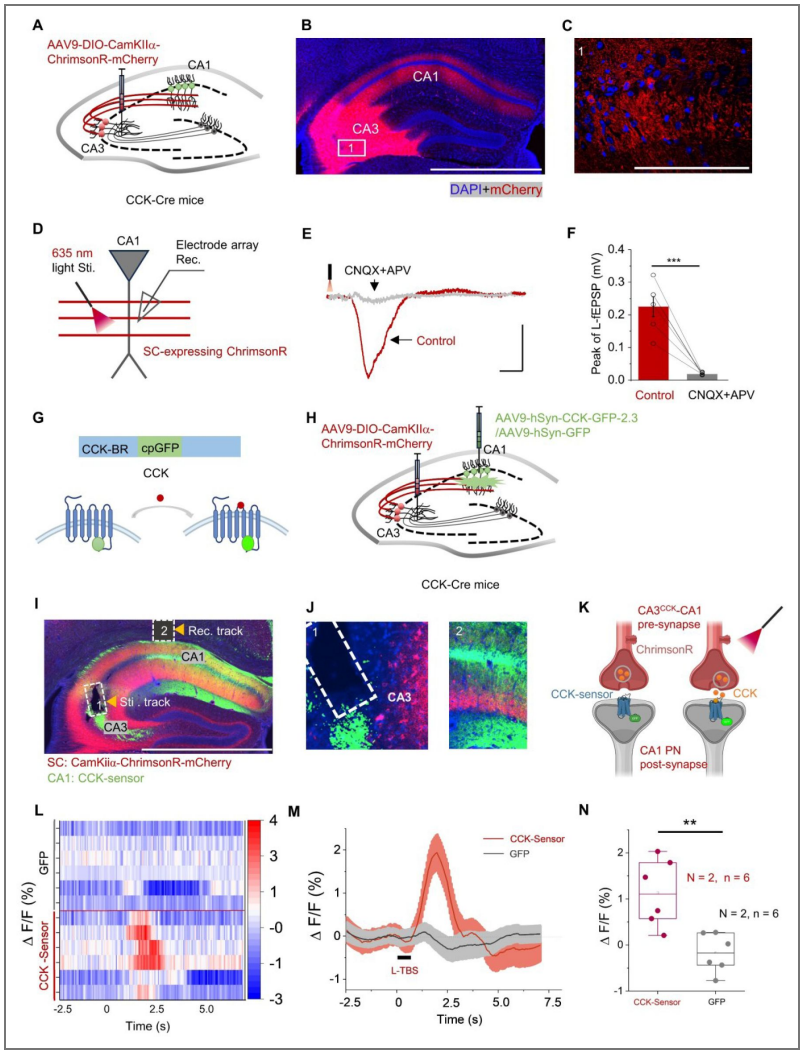

Figure 2. Excitatory CA3 neurons secret the neuropeptide CCK.

(A) Schematic diagram illustrating the viral injection strategy. AAV9-DIO-CaMKIIα-mCherry (5.0 × 10^{12} vg/mL, 250 nL) was injected into the CA3 region of CCK-Cre mice to selectively label excitatory CCK-expressing neurons. **(B)** Representative fluorescence image showing viral expression in the hippocampal CA3 region and labeled projections to the CA1 area. Scale bar, 1000 μm. **(C)** Higher-magnification image of the boxed region in (B), highlighting labeled CA3 axons projecting to CA1. Scale bar, 50 μm. **(D)** Schematic illustrating the experimental configuration for hippocampal slice electrophysiological recordings. **(E)** Representative light-evoked field excitatory postsynaptic potentials (L-fEPSPs) recorded from CA1 following optical stimulation of CA3 CCK-positive Schaffer collateral (SC) projections, shown before and after application of the glutamatergic receptor antagonists CNQX and APV. Scale bars, 0.2 mV and 10 ms. **(F)** Quantitative analysis of glutamatergic synaptic transmission mediated by CA3 CCK-positive projections to CA1, summarized across recordings. **(G)** Schematic illustration of the CCK sensor principle. Binding of the CCK ligand to the genetically encoded sensor induces a conformational change that results in altered fluorescence intensity. **(H)** Experimental schematic showing co-injection of AAV9-hSyn-CCK sensor 2.3 (5.75 × 10^{12} vg/mL, 200 nL) and AAV9-CaMKIIα-DIO-ChrimsonR-mCherry (5.0 × 10^{12} vg/mL, 250 nL) into the CA1 and CA3 regions, respectively, followed by optogenetic stimulation and fiber photometry recording. **(I)** Representative fluorescence image showing expression of the CCK sensor in the CA1 region surrounding the optical fiber tip (left; scale bar, 1000 μm) and ChrimsonR-expressing CA3-CA1 projections in CCK-Cre mice (right). **(J)** Higher-magnification images illustrating the optical stimulation site in CA3 and the photometry recording site in CA1. **(K)** Schematic model depicting activity-dependent release of CCK from CA3 presynaptic terminals onto CA1 neurons. **(L)** Heatmap representation of calcium-dependent fluorescence responses following optogenetic long theta-burst stimulation (L-TBS) in control GFP-expressing mice (upper; N = 3 animals, n = 6 trials) and CCK sensor-expressing mice (lower; N = 3 animals, n = 6 trials). **(M)** Averaged ΔF/F fluorescence responses evoked by optogenetic stimulation (635 nm L-TBS) in GFP and CCK sensor groups (N = 3 animals per group, n = 6 trials each). **(N)** Quantification of the mean fluorescence response in CCK-Cre mice, calculated as the averaged ΔF/F within 3 s following L-TBS. *p < 0.05, **p < 0.01, ***p < 0.001; ns not significant. Data are reported as mean ± SEM.

adjustment; $F_{1,10}$ = 1.88, p = 0.20; Training (Δ *F*/*F*): O1 0.27 ± 0.07 % v.s. O2 0.31 ± 0.08 %, p = 0.91; Testing (Δ *F*/*F*): O1 0.27 ± 0.09 % v.s. O2" 0.41 ± 0.12 %, p = 0.04), which implies that excitatory $CA3^{CCK}$ neurons are critical for specific spatial memory and learning.

Furthermore, we examined whether the excitatory $CA3^{CCK}$ neurons are necessary for performing the MWM paradigm (Figure 3G). Intriguingly, in the naive training (trial 1), a robust and persistent Ca^{2+} responses were observed during the initial learning (Figure 3H and Figure 3I). Nevertheless, after the completion of training, $CA3^{CCK}$ neurons produced a relatively smaller Ca^{2+} signal on the training day 3 with an averaged escape latency of < 10 s to locate the hidden platform (Figure 3H and Figure 3J; Figure 3K: Paired sample t-test, df = 5, t = 2.80; Trial 1: 1.32 ± 0.74 % v.s. Trial 9: 0.75 ± 0.35 %, p = 0.038), this result further supports the conclusion that excitatory $CA3^{CCK}$ neurons plays a direct role in the animals' accurate spatial learning and memory formation.

Chemogenetic inhibition of the excitatory $CA3^{CCK}$-CA1 pathway impairs behavioral tasks

Next, to further confirm the necessity of excitatory $CA3^{CCK}$-CA1 pathway for performance of the hippocampal-dependent behaviors. We adopted the chemogenetic approach, which is a powerful technique for specific disturbance of neuronal activity through virus-mediated DREADD expression in combination with its agonist clozapine N-oxide (CNO) (Gomez et al., 2017), to specifically target the excitatory $CA3^{CCK}$ neurons. Firstly, we injected the Cre dependent AAV expressing the inhibitory DREADD (hM4DGi) to infect the excitatory $CA3^{CCK}$ neurons and AAV carrying mCherry as control (Figure 4A) and implanted the drug cannular upon the CA1 area. The AAV exhibits high specificity for interacting the CCK positive neurons in the CA3 area (91.50 ± 2.24 %; sFigure 3). Four weeks after the AAV injection and expression (Figure 4B), we conducted the MWM task in the two groups of mice to assess the role of CA1-projecting $CA3^{CCK}$ neurons in hippocampus-dependent spatial learning (Figure 4C). Thus, we delivered the CNO (300 nl; 10 μM) via the cannulas to inhibit CCK^{+} CA3-CA1 projections upon the area CA1 before conducting the MWM. Then, two groups of mice were subjected to the visible platform task to evaluate their swimming capability. Both groups of mice displayed comparable swimming speed and the speed time in finding the visible platform (Figure 4D; two sample t-test, df = 18, t = 0.22, HM4D(Gi): 24.3 ± 1.66 cm/s v.s. mCherry: 23.8 ± 1.52 cm/s, p = 0.83. Figure 4E; two sample t-test, df = 18, t = 1.09, HM4D(Gi): 30.86 ± 2.587 s v.s. mCherry: 34.21 ± 2.12 s, p = 0.29). During the hidden platform task, the mice only expressing mCherry gradually spent less time in locating the platform compared to the mice infected with hM4D(Gi) (Figure 4F; two-way mixed ANOVA, Bonferroni adjustment; $F_{4,15}$ = 1.24, p = 0.34; HM4D(Gi): 24.18 ± 4.36 s v.s. mCherry: 15.12 ± 2.13 s on day 5, p = 0.003). Additionally, the control mice showed higher percentage on the target quadrant on the memory retention day, while lower percentage of the occupancy in experimental mice (Figure 4G-H; two-way mixed ANOVA, Bonferroni adjustment; $F_{3,16}$ = 1.19, p = 0.34; HM4D(Gi): 27.91 ± 2.75 % v.s. mCherry: 42.31 ± 3.82 % in quadrant 3, p = 0.02). These results demonstrated that excitatory $CA3^{CCK}$-CA1 pathway is required for animals to perform adequately in spatial learning. Additionally, high-frequency electrical stimulation fails to induce LTP in the CA3-CA1 pathway in both CCK-KO and CCK-BR-KO mice, indicating that CCK-dependent synaptic plasticity in this circuit is primarily mediated by CCK-B receptors.

In the NOL task (Figure 4I), both groups of mice showed equal motivation to explore objects (Figure 4J; two sample t-test, df = 18, t = −0.31, hM4D(Gi): 81.18 ± 9.14 s v.s. mCherry: 85.35 ± 9.67 s, p = 0.76). Compared with the control mice, the experimental group was unable to distinguish the novel and familiar object location in the test phase, and presented low discrimination ratio (Figure 4K; two-way mixed ANOVA, Bonferroni adjustment; $F_{1,18}$ = 4.58, p = 0.04; hM4D(Gi): Familiar 40.83 ± 5.27 s v.s. Novel: 43.46 ± 7.40 s, p = 0.66; mCherry 34.38 ± 3.58 s v.s. Novel: 55.35 ± 6.11 s, p = 0.003. Figure 4L; two sample t-test, df = 18, t = 0.77, hM4D(Gi): −0.003 ± 0.09 v.s. mCherry: 0.22 ± 0.06, p = 0.03), indicating suppression of excitatory $CA3^{CCK}$-CA1 pathways impaired the spatial memory. Taken together, we can conclude that excitatory $CA3^{CCK}$ neuron is an essential and functional component in the hippocampal system.

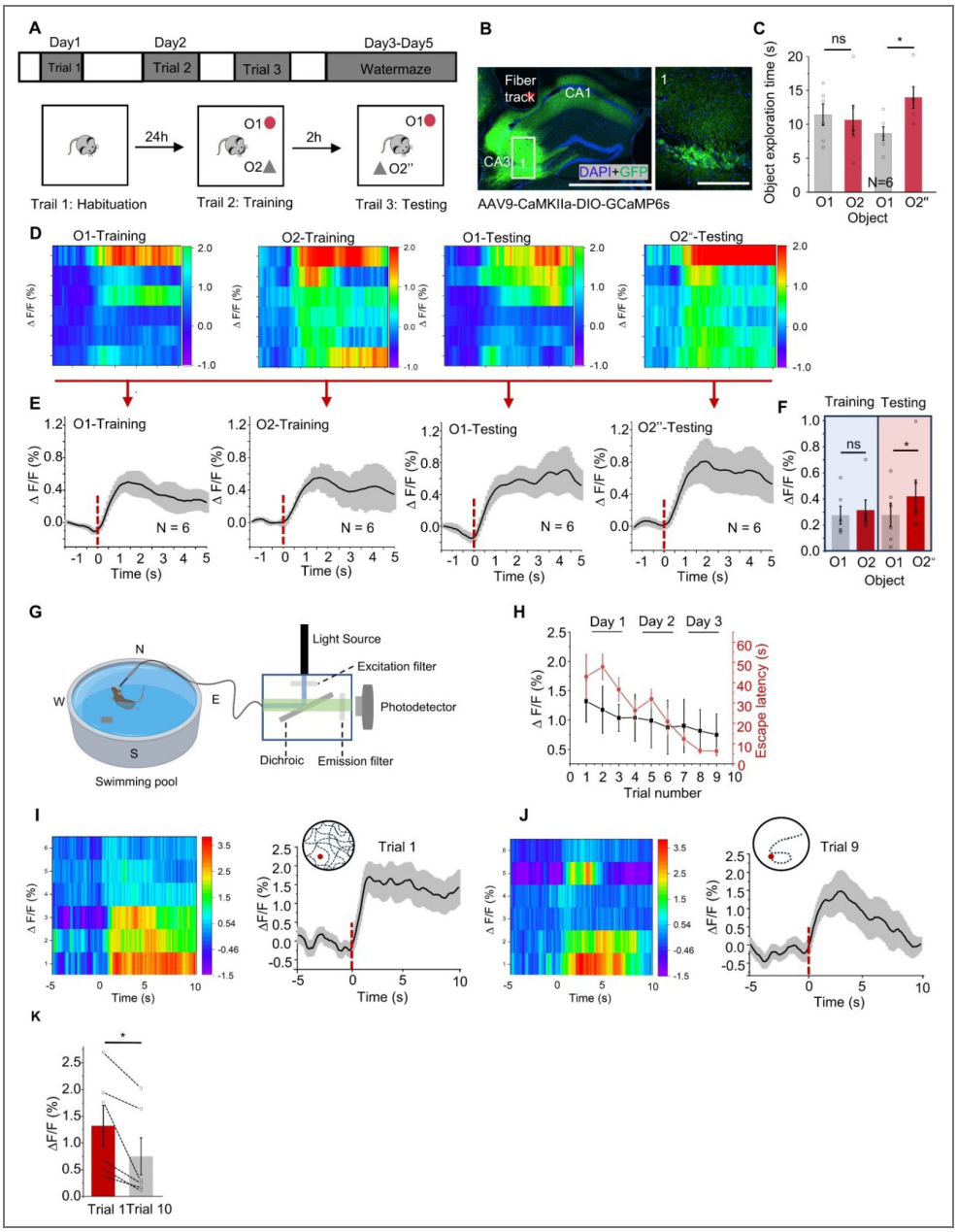

Figure 3. **CA3^{CCK} neurons fire actively during hippocampal-dependent tasks.**

(A) Schematic overview of the behavioral paradigms used in this study, including the novel object location (NOL) task and the Morris water maze (MWM) task. **(B)** Representative fluorescence images showing viral injection into the CA3 region and expression of GCaMP6s in CCK-positive neurons of CCK-Cre mice following injection of AAV9-CaMKIIα-DIO-GCaMP6s (5.0 × 10^{12} vg/mL, 300 nL). Scale bars, 1000 μm (left) and 100 μm (right). **(C)** Behavioral performance during the NOL task showing that mice spent significantly more time interacting with the object placed in a novel location compared with the familiar location. **(D)** Heatmap representation of ΔF/F fluorescence traces from a representative mouse during the training and testing phases of the NOL task (N = 6 mice). **(E)** Averaged ΔF/F fluorescence traces from all mice (N = 6), aligned to the onset of object exploration. **(F)** Mean GCaMP6s fluorescence signals of CA3 CCK-expressing neurons during object exploration bouts in training and testing trials, quantified as the average ΔF/F within 1.5 s following exploration onset. **(G)** Schematic illustration of the experimental setup for calcium imaging during the Morris water maze task. **(H)** Representative plot showing the relationship between normalized ΔF/F signals (black) and escape latency (red) across training trials in the MWM task. **(I)** Heatmap and mean GCaMP6s fluorescence signals during the initial learning phase (trial 1) of the MWM task. **(J)** Heatmap and mean GCaMP6s fluorescence signals during the well-trained phase (trial 9) of the MWM task. **(K)** Summary quantification of ΔF/F signals comparing trial 1 and trial 9, calculated as the average fluorescence within 10 s following trial onset. *p < 0.05, **p < 0.01, ***p < 0.001; ns, not significant. Data are reported as mean ± SEM.

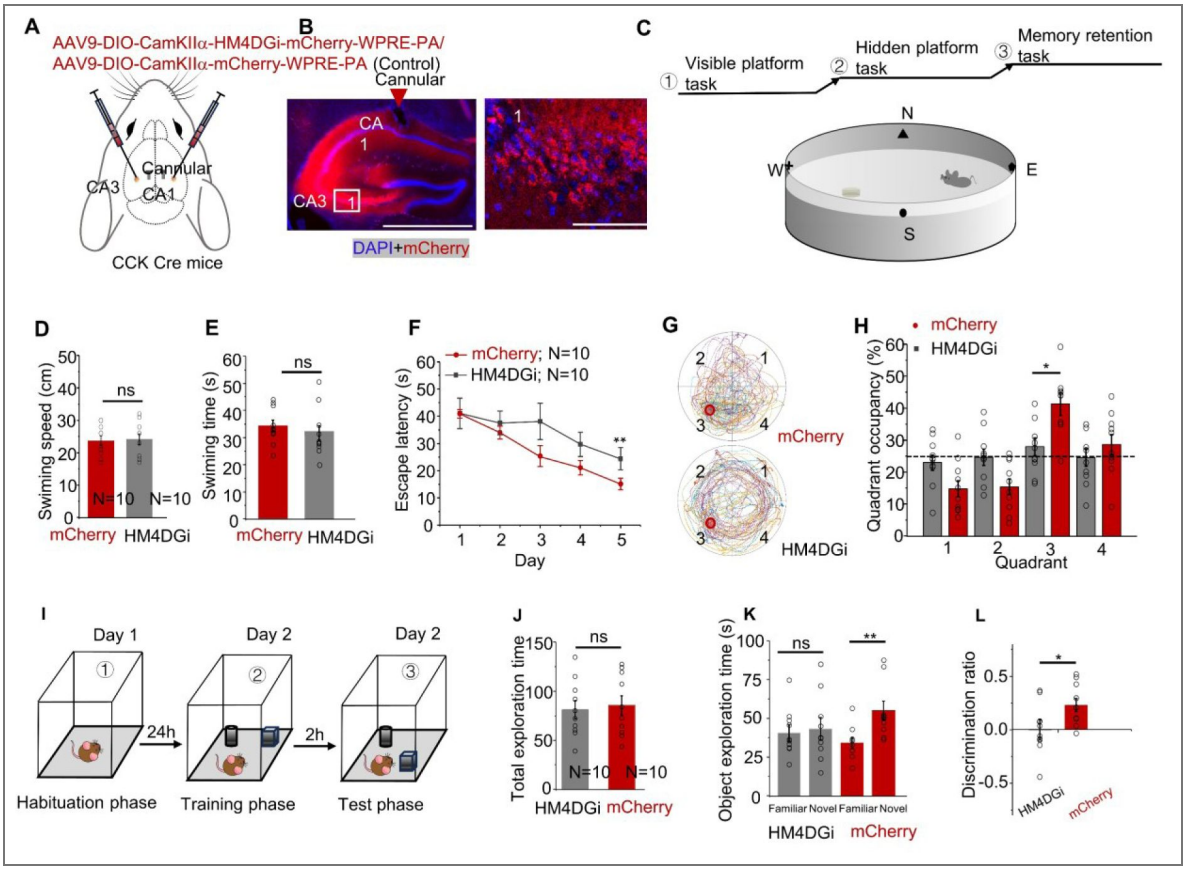

Figure 4. Chemogenetic inhibition of the excitatory CA3^{CCK}-CA1 pathway impairs behavioral tasks.

(A) Schematic illustrating Cre-dependent viral labeling and chemogenetic manipulation of CA3–CA1 projections in CCK-Cre mice. AAV9-CaMKIIα-DIO-hM4D(Gi)-mCherry (6.5 × 10¹² vg/mL, 300 nL) or control AAV9-hSyn-DIO-mCherry (6.5 × 10¹² vg/mL, 300 nL) was injected to selectively target excitatory CCK-expressing neurons. **(B)** Representative fluorescence image showing viral expression in the CA1 region with the corresponding cannula track. A higher-magnification image of the boxed area is shown on the right. Scale bars, 1000 μm (left) and 100 μm (right). **(C)** Schematic of the Morris water maze (MWM) task. The hidden platform was located in the southwestern (SW) quadrant (quadrant 3). **(D)** Quantification of swimming speed during the visible platform task, showing no significant differences between control and hM4D(Gi)-expressing mice. **(E)** Quantification of latency to locate the visible platform, indicating comparable sensorimotor performance between groups. **(F)** Escape latency across training days during the hidden platform phase of the MWM, comparing control and hM4D(Gi) groups. **(G)** Representative swimming trajectories of control and hM4D(Gi)-expressing mice during the spatial probe trial. **(H)** Percentage of total time spent in each quadrant during the probe test, showing reduced preference for the target quadrant in hM4D(Gi)-expressing mice. **(I)** Schematic of the novel object location (NOL) task (see Methods for details). **(J)** Total object exploration time during the NOL task, showing no significant difference between groups. **(K)** Control mice expressing mCherry exhibited a stronger preference for the object in the novel location compared with hM4D(Gi)-expressing mice. **(L)** Quantification of discrimination index demonstrating a significant reduction in spatial discrimination performance in hM4D(Gi)-expressing mice compared with controls. ∗p < 0.05, ∗∗p < 0.01, ∗∗∗p < 0.001; ns, not significant. Data are reported as mean ± SEM.

Chemogenetic inhibition of the excitatory CA3^{CCK}-CA1 pathway attenuates LTP formation

Since the LTP in the hippocampus is commonly considered a key cellular mechanism that underlies spatial learning and memory (Ge et al., 2010). To confirm whether excitatory CA3^{CCK}-CA1 pathway are directly involved in LTP formation, we further conducted the electrophysiological recording in *vitro*. Four weeks after the AAV injection and expression (Figure 5A-B), hippocampal slices were subjected to electrophysiological recording to test the effect of CNO on the neuroplasticity of excitatory CA3^{CCK}-CA1 pathway (Figure 5C).

After the baseline recording, the slope of fEPSPs decreased gradually with the CNO treatment while no significant changes were observed in controls (Figure 5D-E; two-way mixed ANOVA, Bonferroni adjustment; $F_{1,13} = 78.32$, $p < 0.001$; hM4D(Gi): Pre_{ex} 100.42 ± 0.18 % v.s. $Post_{ex}$ 78.07 ± 1. 52 %, $p < 0.001$; mCherry: Pre_{ctrl} 100.15 ± 0.48 % v.s. $Post_{ctrl}$ 98.90 ± 2.90 %, $p = 0.60$, $Post_{ex}$ v.s. $Post_{ctrl}$, $p < 0.001$), indicating that neuronal activities of the excitatory CA1-projecting CA3^{CCK} neurons were remarkably suppressed. Then, we further employed the E-TBS protocol for the LTP induction under this condition (Figure 5F). Intriguingly, the extent of LTP formation in the slices expressing hM4D(Gi) was significantly smaller than those in the control group (Figure 5G-H; two way mixed ANOVA, Bonferrori adjustment; $F_{1,13} = 9.46$, $p = 0.01$; HM4D(Gi): Pre_{ex} 99.65 ± 0.31 % v.s. $Post_{ex}$ 111.52 ± 2.40 %, $p < 0.001$, mCherry: Pre_{ctrl} 100.41 ± 0.29 % v.s. $Post_{ctrl}$ 125.17 ± 3.43 %, $p = 0.001$, $Post_{ex}$ v.s. $Post_{ctrl}$, $p = 0.005$), hinting that CA3^{CCK} neurons are involved in the maintenance of hippocampal neuroplasticity.

RNA interference of excitatory CA3^{CCK} expression impairs hippocampal functions

Next, to verify whether neuropeptide CCK in excitatory CA3^{CCK} neurons are also involved in spatial learning and memory, RNA interference (RNAi) strategy was utilized to downregulate CCK expression in CA3^{CCK} neurons (Figure 6A). We thus injected AAV9-CamkIIα-DIO-mCherry-shRNA (CCK) into area CA3 to knockdown target gene and AAV9-CamkIIα-DIO-mCherry-shRNA (Scramble) as control. The experimental group was Cre on anti-CCK to knock down the expression of CCK in the area CA3 of CCK Cre mice, while the control group was Cre on anti-scramble. We confirmed the expression of shRNAs in the hippocampus at 4 weeks after AAV injection (Figure 6B). Moreover, we further verified that anti-CCK shRNAs faithfully downregulated CCK mRNA levels *in vivo* by using the qPCR technique and histology method (Figures 6C; two sample t-test, df = 10, t = 4.95, anti-scramble 100 ± 7.03 % v.s. anti-CCK 58.73 ± 7.23 %, P = 0.001; sFigure 4A-B; two sample t-test, df = 16, t = 6.23, anti-scramble 52.44 ± 2.64 cells v.s. anti-CCK 19.12 ± 4.45 %, P < 0.001). Subsequently, we conducted the MWM task in the two groups of mice to assess the role of CA1-projecting CA3^{CCK} neurons in the hippocampus-dependent spatial learning (Figure 6D).

The two groups of mice injected with anti-CCK and anti-scramble showed comparable swimming speed (Figure 6E; two sample t-test, df = 18, t = −0.40, anti-CCK: 23.3 ± 2.75 cm/s v.s. anti-scramble: 24.1 ± 1.41cm/ s, p = 0.69) and swimming time in locating the visible platform above the water surface of the swimming pool (Figure 6F; two sample t-test, df = 18, t = −0.51, anti-CCK: 33.4 ± 2.21 s v.s. anti-scramble: 34.9 ± 1.93 s, p = 0.62). Then, mice infected with the anti-CCK showed deficits in spatial learning during the 5 days training (Figure 6G; two way mixed ANOVA, Bonferrori adjustment; $F_{4,15} = 0.30$, $p = 0.88$; anti-CCK 25.48 ± 2.12 s v.s. anti-scramble 18.05 ± 3.10 s on day 5, $p = 0.007$), and also exhibited deficiency in memory retention (Figure 6H-I; two way mixed ANOVA, Bonferrori adjustment; $F_{3,16} = 1.20$, $p = 0.34$; anti-CCK 28.38 ± 1.78 % v.s. anti-scramble 35.76 ± 3.68 % in quadrant 3, p = 0.03). These results suggest that knockdown of CCK expression in area CA3 attenuates spatial learning ability.

In another spatial learning protocol, the novel object location (NOL) task (Figure 6J), two groups of mice exhibited equal motivation to explore objects (Figure 6K; two sample t-test, df = 18, t = 0.28, anti-CCK: 83.82 ± 5.85 s v.s. anti-scramble: 81.22 ± 7.25 s, p = 0.78). Compared with the control mice (anti-scramble), the mice infected with anti-CCK failed to distinguish between the novel and

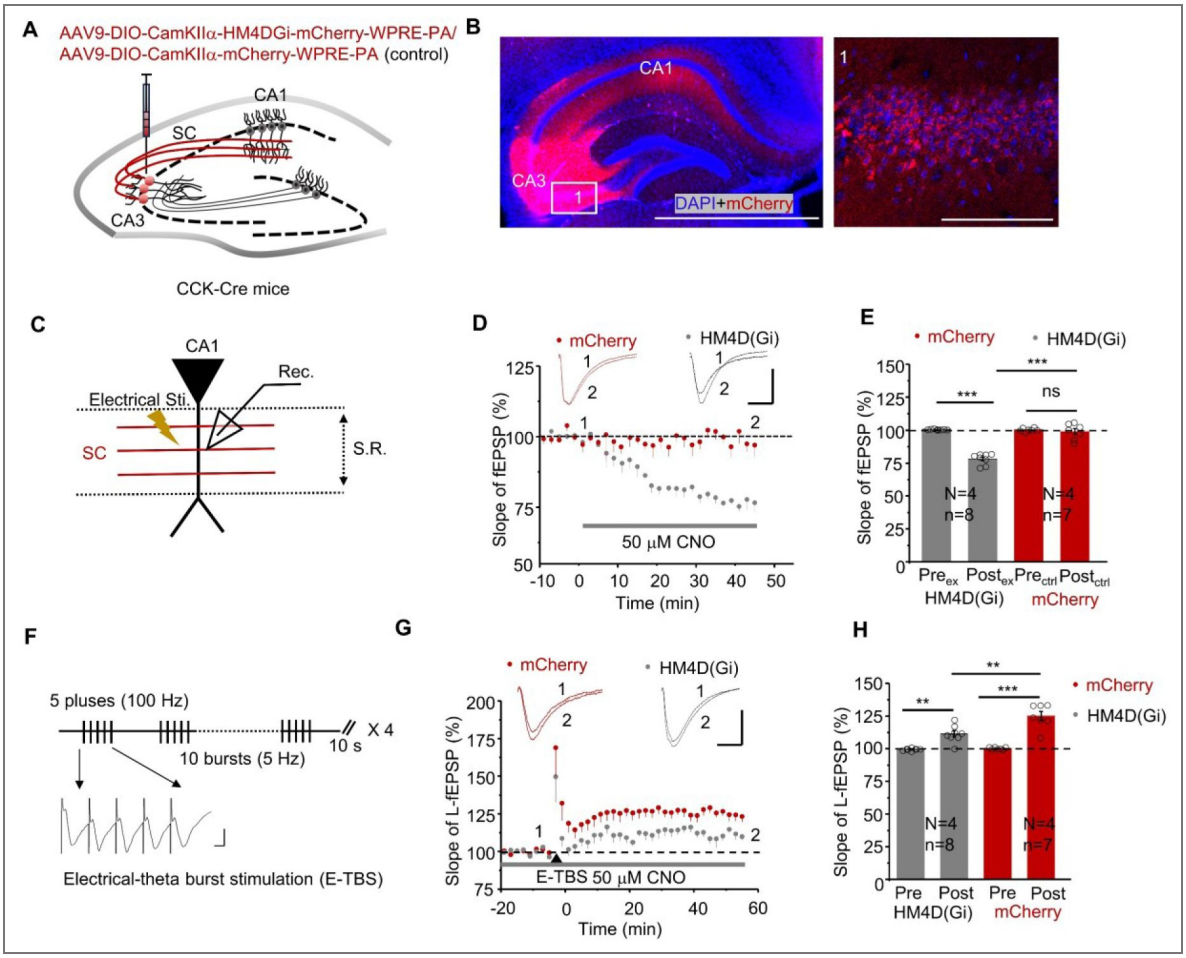

Figure 5. Chemogenetic inhibition of the excitatory CA3^{CCK}-CA1 pathway impairs LTP formation.

(A) Schematic illustrating the viral injection strategy. AAV9-CaMKIIα-DIO-hM4D(Gi)-mCherry (5.0 × 10^{12} vg/mL, 300 nL) or control AAV9-hSyn-DIO-mCherry (5.0 × 10^{12} vg/mL, 300 nL) was injected into the CA3 region of CCK-Cre mice to selectively target excitatory CCK-expressing neurons. **(B)** Representative fluorescence images showing viral expression in the hippocampal CA3 region and labeled projections to the CA1 area. A higher-magnification image of the boxed region is shown on the right. Scale bars, 1000 μm (left) and 100 μm (right). **(C)** Schematic illustration of the hippocampal slice electrophysiological recording configuration. **(D)** Representative electrically evoked field excitatory postsynaptic potentials (E-fEPSPs) recorded in CA1 following stimulation of CA3 Schaffer collateral inputs before and after application of clozapine-N-oxide (CNO). Chemogenetic inhibition significantly reduced E-fEPSP amplitude in slices expressing hM4D(Gi) compared with mCherry-expressing controls. Scale bars, 0.2 mV and 10 ms. **(E)** Quantification of E-fEPSP responses showing reduced synaptic transmission in hM4D(Gi)-expressing slices relative to control slices following CNO application. **(F)** Schematic of the electrical theta-burst stimulation (E-TBS) protocol used to induce long-term potentiation (LTP). **(G)** Representative traces showing that LTP induction was attenuated in hM4D(Gi)-expressing slices compared with mCherry controls. Scale bars, 0.2 mV and 10 ms. **(H)** Summary quantification of E-fEPSP responses following E-TBS, demonstrating significantly reduced LTP in the hM4D(Gi) group relative to controls. ∗p < 0.05, ∗∗p < 0.01, ∗∗∗p < 0.001; ns, not significant. Data are reported as mean ± SEM.

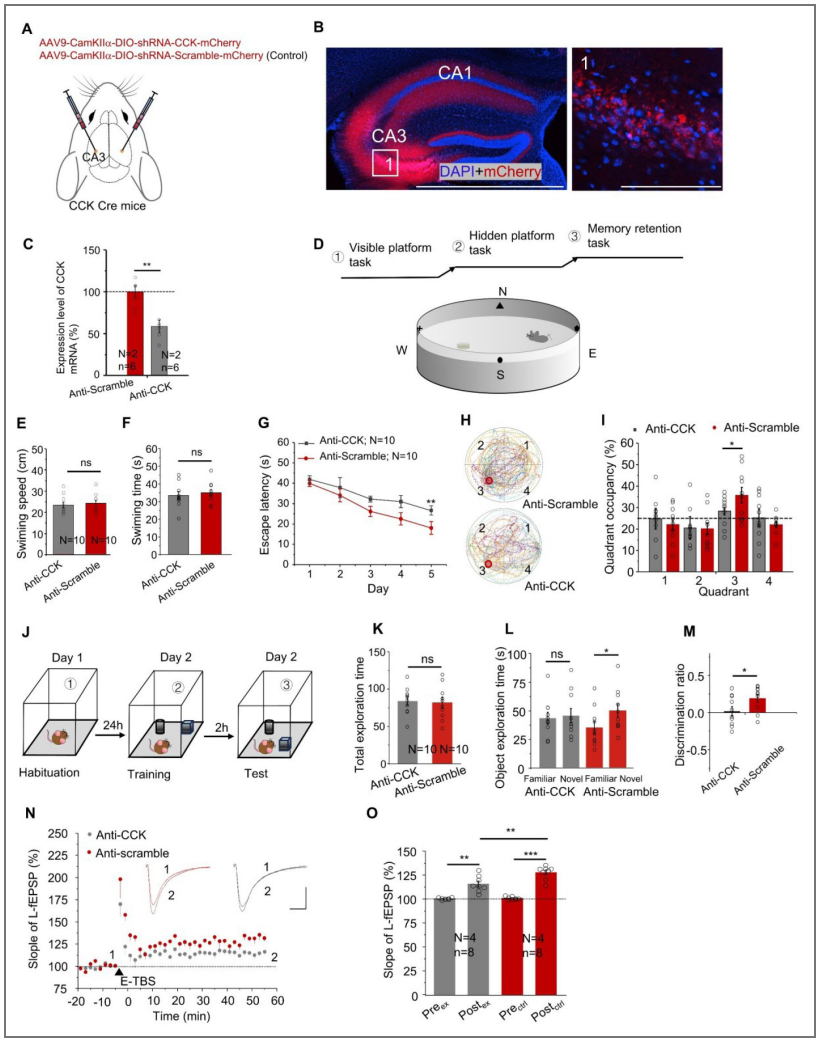

Figure 6. RNA interference of excitatory CA3^{CCK} expression attenuates hippocampal functions.

Schematic illustrating the viral strategy for CCK knockdown in CA3 CCK-expressing neurons. CCK-Cre mice received injections of AAV9-CaMKIIα-DIO-(mCherry-bGH pA-U6)-shRNA-CCK or control AAV9-CaMKIIα-DIO-(mCherry-bGH pA-U6)-shRNA-Scramble (5.0 × 10^{12} vg/mL, 300 nL) into the CA3 region. **(B)** Representative fluorescence images showing viral expression in the hippocampal CA3 region and labeled projections to the CA1 area. A higher-magnification image of the boxed region is shown on the right. Scale bars, 1000 μm (left) and 100 μm (right). **(C)** Quantification of CCK mRNA expression in the CA3 region of CCK-Cre mice infected with anti-CCK shRNA or scramble control shRNA, confirming efficient knockdown of CCK expression. **(D)** Schematic illustration of the hippocampal slice electrophysiological recording configuration. **(E)** Quantification of swimming speed during the visible platform task of the Morris water maze (MWM), showing no significant difference between anti-CCK and anti-scramble groups. **(F)** Quantification of latency to locate the visible platform, indicating intact sensorimotor performance in both groups. **(G)** Escape latency during the hidden platform training phase of the MWM for anti-CCK and anti-scramble groups. **(H)** Representative swimming trajectories of anti-CCK and anti-scramble mice during the spatial probe trial of the MWM. **(I)** Percentage of total time spent in each quadrant during the probe test, showing reduced preference for the target quadrant in anti-CCK mice compared with controls. **(J)** Schematic of the novel object location (NOL) task (see Methods for details). **(K)** Total object exploration time during the NOL task, showing no significant difference between anti-CCK and anti-scramble groups. **(L)** Control mice expressing scramble shRNA exhibited a greater preference for the object in the novel location compared with anti-CCK mice. **(M)** Quantification of discrimination index demonstrating significantly reduced spatial discrimination performance in anti-CCK mice relative to scramble controls. **(N)** Representative traces showing that long-term potentiation (LTP) induced by electrical stimulation was attenuated in hippocampal slices expressing anti-CCK shRNA compared with scramble controls. Scale bars, 0.2 mV and 10 ms. **(O)** Summary quantification of electrically evoked field excitatory postsynaptic potentials (E-fEPSPs) following LTP induction, demonstrating reduced synaptic potentiation in the anti-CCK group relative to controls. ∗p < 0.05, ∗∗p < 0.01, ∗∗∗p < 0.001; ns, not significant. Data are reported as mean ± SEM.

familiar object location in the test phase, and displayed low discrimination ratio (Figure 6L; two-way mixed ANOVA, Bonferrori adjustment; $F_{1,18} = 2.97$, $p = 0.10$; anti-CCK: Familiar 42.63 ± 5.21 s v.s. Novel: 44.87 ± 6.33 s, $p = 0.67$; anti-scramble: Familiar 34.41 ± 5.30 s v.s. Novel: 49.22 ± 8.87 s, $p = 0.01$. Figure 6M; two sample t-test, df = 18, t = −2.0, anti-CCK: 0.02 ± 0.06 v.s. anti-scramble: 0.19 ± 0.05, $p = 0.04$), indicating that downregulation of CCK expression in area CA3 was sufficient to impair spatial memory. Taken together, these results support our hypothesis that excitatory CCK acts as a functional neuromodulator in the hippocampal system.

Additionally, for the electrophysiology recording, E-TBS adequately induced LTP at CA3-CA1 synapses in control slices containing the anti-scramble shRNAs, but the same protocol elicited remarkably smaller LTP on slices with anti-CCK shRNA targeting the sequences of CCK gene (Figures 6N-O; two way mixed ANOVA, Bonferrori adjustment; $F_{1,14} = 10.06$, $p = 0.007$; Pre_{ctrl}: 100.93 ± 0.57 % v.s. $Post_{ctrl}$: 127.78 ± 2.47 %, $p < 0.001$; Pre_{ex}: 100.44 ± 0.34 % v.s. $Post_{ex}$: 115.76 ± 2.96 %, $p < 0.001$; $Post_{ctrl}$ v.s. $Post_{ex}$, $p = 0.008$). Moreover, we noticed that the amplitude of the electrically evoked fEPSPs in anti-CCK group is similar to those of the control group (Figures 6N, insert), suggesting normal neurotransmission in hippocampal slices from both groups. Therefore, the impairment of LTP is likely due to the reduced expression of CCK in CA1-projecting $CA3^{CCK}$ terminals which impaired the neuromodulation.

Discussion

In the present study, we reported the distribution profile of CCK positive neurons in the dorsal hippocampus, a key brain region associated with spatial memory formation and transformation (Martin and Clark 2007). Although the role of inhibitory CCK neurons is well studied in the hippocampus, the function of excitatory CCK neurons is still unclear. Optogenetic activation of the CCK inhibitory populations produces a prominent IPSC and controls the input and output gain of CA1 pyramidal neurons, and this kind of modulation is mediated by the presynaptic CB1 receptors (Hartzell et al., 2018). A recent study uncovered that systemic activation of CCK-GABA neurons minimally affects emotion but significantly enhances cognition and memory (Whissell et al., 2019). In our study, we combined the Ai14::CCK Cre mice and immunochemistry method to show the distribution of CCK positive neurons in the hippocampus. Moreover, we adopted the pharmacological approach to diminish the tendency for light-evoked fEPSPs of excitatory CA1-projecting $CA3^{CCK}$neurons. Additionally, using the patch clamp technique to record the EPSP of these neurons also can directly validate this conclusion. Due to technical limitations at the current stage, we were unable to perform whole-cell recordings or pharmacological manipulations using CCK receptor antagonists. In future studies, the application of these approaches to directly record and selectively block EPSPs from excitatory CCK neurons in the hippocampus will further strengthen and validate our conclusions. Importantly, to further improve cell-type specificity, we propose an intersectional genetic strategy using CCK-IRES-Cre × VGlut1-Flp mice combined with a Cre-On/Flp-On (Con/Fon) AAV, which would restrict expression exclusively to excitatory CCK-expressing neurons and eliminate potential contributions from inhibitory CCKL cells. This approach will be implemented in future studies to refine circuit specificity. To our knowledge, this is the first study that demonstrated the function of excitatory CCK neurons in the hippocampus.

Additionally, to fully validate the involvement of excitatory CA1-projecting $CA3^{CCK}$ neurons in hippocampal processing involving learning and neuroplasticity, we used the chemogenetic technique to examine the function of $CA3^{CCK}$ neurons. Interestingly, we found that specific inhibition of these neurons significantly impaired the CA1-CA3 LTP and attenuated spatial learning. Many studies have also demonstrated that neurotransmitters facilitate the hippocampal plasticity and further modulate the behavior performance (Birthelmer et al., 2003; Ohta et al., 2003; Lopes et al., 2002), because deficiency of neurotransmitters in the CNS is known to be able to decrease the extent of synaptic transmission in the CA3-CA1 pathway. For instance, Mlinar reported that endogenous 5-hydroxytryptamine (5-HT) potentiates the LTP in the hippocampus and its positive effects on cognitive performance (Mlinar et al., 2015). Also, another study used a viral-mediated approach to delete brain-derived neurotrophic factor (BDNF) specifically in CA3-CA1 pathway, and further demonstrated that presynaptic and postsynaptic BNDF are essential for

LTP induction and maintenance, as well as contextual memory impairments (Mohajerani et al., 2007). In this study, we used RNA interference technique (RNAi) to fully characterize the function of $CA3^{CCK}$ neurons. Intriguingly, the knock down of CCK expression significantly impaired LTP formation at excitatory CA1-projecting $CA3^{CCK}$ synapses and further affected the hippocampus dependent-spatial learning and memory. Interestingly, an earlier study demonstrated that intraperitoneal injection of exogenous CCK-4 significantly improved performance in hippocampus-dependent spatial learning tasks in both CCK gene knockout (CCK-KO) mice and Alzheimer's disease (AD) mouse models (Zhang et al., 2024). These findings suggest that enhancing CCK signaling can ameliorate hippocampal dysfunction at both the behavioral and synaptic plasticity levels. Therefore, we established the essential role of CCK as an active neuromodulator that regulates hippocampal plasticity and its dependent behaviors (Figure 7).

Establishing a causal link between neural plasticity and spatial learning is crucial for understanding the status of $CA3^{CCK}$ neurons in the hippocampus. Our investigation verified that $CA3^{CCK}$ neurons modulate hippocampal long-term plasticity in a homosynaptic manner, and their activity underlies spatial learning and memory formation. We demonstrated that the $CA3^{CCK}$ projections to the CA1 region are required and sufficient to induce the LTP at CA3-CA1 synapses. In the behavioral setup, we also observed that the calcium response of CA1-projecting $CA3^{CCK}$ neurons increased during the exploration. The Ca^{2+} activities were also raised throughout the MWM task. Nevertheless, perturbation of the activities of $CA3^{CCK}$ neurons impaired spatial learning both in the NOL task and MWM task. It was likely that the CA3 input to the CA1 conveys spatial information. Thus, we can conclude that $CA3^{CCK}$ neurons may specifically regulate the hippocampal state and plasticity during behavioral performance.

Finally, further experimental works could be undertaken to investigate the function of $CA3^{CCK}$ neurons. For instance, the change of CCK concentration during the light high frequency stimulation of CA1-projecting $CA3^{CCK}$ neurons by using the GPCR-based CCK sensor. Several high-sensitive GPCR-based sensors for detecting the neurotransmitters have been well developed, including the dopamine, norepinephrine, serotonin and acetylcholine. Besides, using a GPCR-based CCK-BR sensor combined with fiber photometry, our previous work demonstrated rapid, activity-dependent CCK release in the hippocampus during object-exploratory behavior, supporting a functional role for hippocampal CCK signaling in cognitive tasks (Su et al., 2023). Given that hippocampal neurons receive CCK-positive projections from multiple brain regions, it remains technically challenging to precisely identify the cellular source of CCK release in CA1 during behavior. Future studies employing selective CCK overexpression in CA3 neurons, together with CCK-BR sensor recordings, may help further delineate the contribution of CA3-derived CCK to hippocampal-dependent behaviors.

Methods

Animals

Adult Cck-IRES-Cre (CCK Cre: *RRID:IMSR_JAX:012706*) mice and Ai14 mice (*RRID:IMSR_JAX:007914*) were used in this study. In behavioral experiments, all male mice were housed in a 12-h light/dark cycle and were provided food and water ad libitum. All experimental procedures were approved by the Animal Subjects Ethics Sub-Committee of the City University of Hong Kong.

Viruses

Adeno-associated virus (AAVs) were purchased from the BrainVTA, Wuhan, China: AAV9-CaMKIIa-DIO-GCaMP6S-WPRE-hGH-pA (PT-0090); AAV9-CaMKIIa-DIO-(mCherry-bGH pA-U6)-shRNA(CCK)-WPRE-hGH pA (PT-9086); AAV9-CaMKIIa-DIO-(mCherry-bGH pA-U6)-shRNA(Scramble)-WPRE-hGH pA (PT-3088); AAV9-CaMKIIa-DIO-hM4D(Gi)-mCherry-WPRE-hGH polyA (PT-1143); AAV9-Syn-DIO-

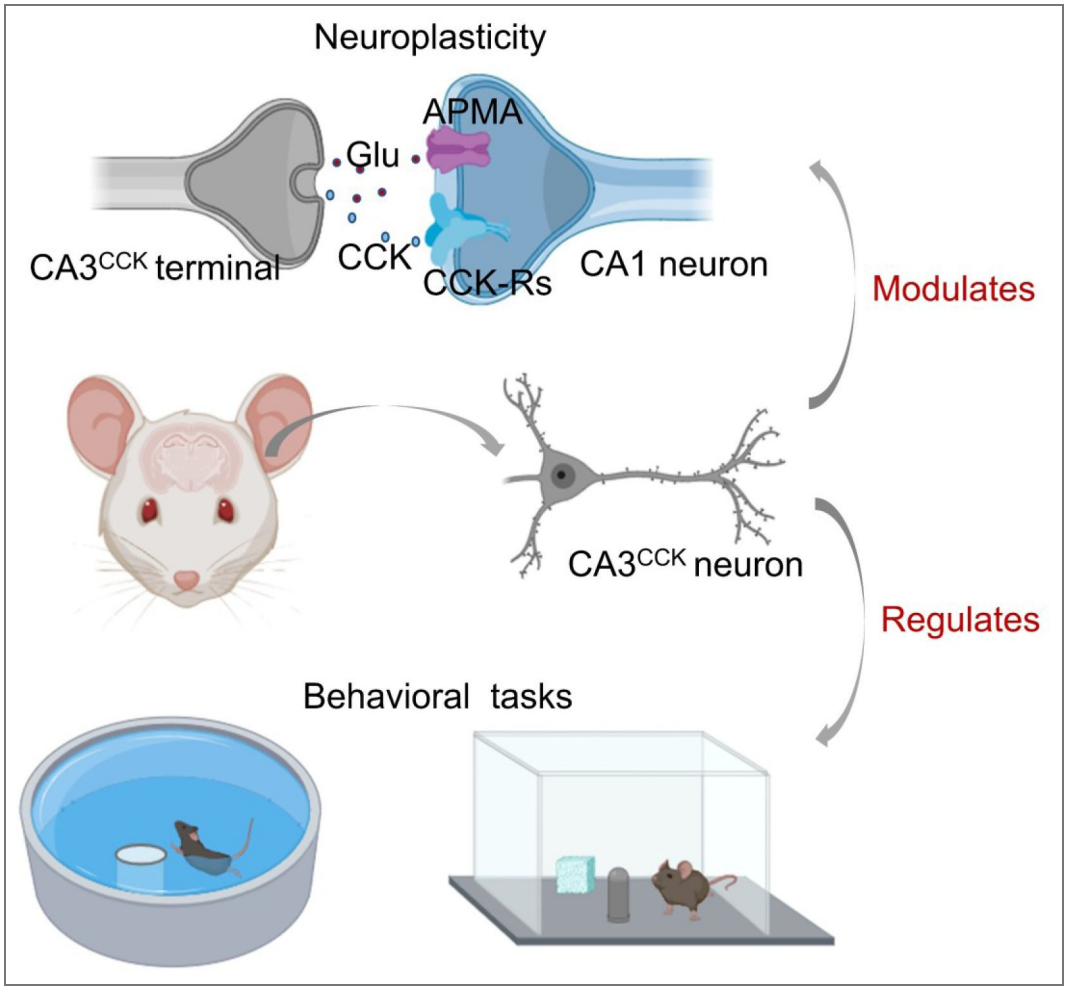

Figure 7. **Summary model illustrating the role of the perforant pathway in regulating spatial memory and hippocampal synaptic plasticity.**

mCherry-WPRE-hGH polyA (PT-0115); AAV9-hSyn-CCK sensor 2.3-GFP; AAV9-hSyn-GFP; Addgene, Cambridge, MA, USA: Retrograde AAV-EF1a-DIO-EYFP (27056). Taitool BioScience, Shanghai, China: AAV9-mCaMKIIa-DIO-ChrimsonR-mCherry-ER2-WPRE-pA (S0728-9).

AAV injection

Adult mice were deeply anesthetized with an intraperitoneal injection of pentobarbital sodium (50 mg/kg; Ceva Santé Animale, France) and secured in a stereotaxic frame. Following a midline scalp incision to expose the skull, the stereotaxic apparatus was adjusted to ensure that bregma and lambda were positioned in the same horizontal plane. A small craniotomy was drilled above the target site, and adeno-associated virus (AAV) was unilaterally delivered into the CA3 region of the hippocampus using a nanoliter injector (Micro4 system, World Precision Instruments) fitted with a quartz glass micropipette. The stereotaxic coordinates relative to bregma were as follows: anteroposterior (AP), −1.70 mm; mediolateral (ML), +2.35 mm; dorsoventral (DV), −1.85 mm.

The viral suspension was infused at a constant rate of 30 nL/min. The total injection volume and viral titer are specified in the corresponding figure legends. To minimize backflow and ensure proper diffusion of the virus, the micropipette was left in place for 5 minutes after completion of the infusion before being slowly withdrawn. After injection, the incision was sutured and treated with erythromycin ointment to prevent infection. Mice were placed on a heating pad until fully recovered from anesthesia and then returned to their home cages for postoperative care.

Brian slice recording

For acute brain slice preparation, mice were deeply anesthetized with 1.4% gaseous isoflurane (Wellona Pharma) and decapitated. The brain was rapidly removed and immediately immersed in ice-cold, oxygenated artificial cerebrospinal fluid (aCSF; 95% OL / 5% CO_2). The aCSF contained (in mM): 124 NaCl, 3 KCl, 1.25 KH_2PO_4, 1.25 $MgSO_4$, 2 $CaCl_2$, 26 $NaHCO_3$, and 10 glucose, with a pH of approximately 7.4. This same aCSF solution was used throughout all subsequent procedures, including tissue dissection, slicing, incubation, and electrophysiological recording. Coronal brain slices (300 μm thickness) containing the hippocampus were prepared using a vibrating microtome (Leica VT1000S). Slices were transferred to oxygenated aCSF and allowed to recover at 32°C before recording.

For electrophysiological recordings, individual hippocampal slices were placed onto a multi-electrode array (MEA) probe and continuously perfused with oxygenated aCSF. Field excitatory postsynaptic potentials (fEPSPs) were recorded using an MEA recording system (Alpha MED Sciences) integrated with a light stimulation module (Inper), allowing for both electrically and optically evoked responses. For electrical stimulation, a designated electrode on the MEA probe served as the stimulating electrode. For optical stimulation, a 2-ms pulse of red light (635 nm) was delivered through a 200-μm-diameter optical fiber positioned over the CA1 region. After stable baseline fEPSP responses were established, input–output (I/O) curves were generated by plotting the slope of the fEPSP against increasing electrical stimulus intensities or optical light intensities. fEPSP slopes were normalized to baseline responses and analyzed using MED Mobius software (Alpha MED Sciences).

Real-time PCR

Tissue samples from the target brain region (hippocampal CA3) were freshly dissected from mice four weeks after AAV-mediated expression of anti-CCK shRNA or scramble control shRNA. Bilateral CA3 tissue was collected for RNA analysis. Total RNA was extracted using TRIzol reagent according to the manufacturer's instructions. Extracted RNA was reverse transcribed into complementary DNA (cDNA) using Maxima Reverse Transcriptase (Thermo Fisher Scientific). Quantitative real-time PCR was performed using a QuantStudio™ 3 Real-Time PCR System (Applied Biosystems) to specifically amplify the CCK transcript. The primer sequences used for CCK amplification were as follows: CCK forward, 5'-AGCGCGATACATCCAGCAG-3'; CCK reverse, 5'-

C-3'. Relative CCK mRNA expression levels were quantified using the comparative threshold cycle (Ct) method (2^−ΔΔCt). Expression levels were normalized to the housekeeping gene GAPDH. Three biological replicates were included for each experimental group.

Morris water maze task

The Morris water maze (MWM) task was conducted according to the protocol described by Vorhees and Williams (2006). The apparatus consisted of a circular pool with a diameter of 122 cm filled with opaque water. All behavioral testing was performed under consistent lighting conditions, with illumination set sufficiently bright to allow accurate video tracking. Prior to hidden platform training, all mice were subjected to a visible platform task to assess visual acuity and swimming ability. During this phase, mice were allowed to locate a visible platform placed above the water surface.

For spatial learning, mice underwent hidden platform training for five consecutive days. During each training session, the platform was submerged below the water surface and remained in a fixed location. Mice were released into the pool and allowed up to 60 s to locate the hidden platform. If a mouse failed to find the platform within the allotted time, it was gently guided to the platform. Mice were allowed to remain on the platform briefly before being returned to their home cages. On day 6, a probe trial was performed to assess spatial reference memory. The platform was removed from the pool, and mice were allowed to swim freely to evaluate memory retention. The former platform location was in the target quadrant (quadrant 3). Swimming trajectories, time spent in each quadrant, and search patterns were recorded and analyzed using MATLAB-based tracking software.

Novel object location task

The novel object location (NOL) task was conducted as previously described (Pérez-García et al., 2016) and consisted of three sequential phases. On day 1, each mouse was habituated to the empty testing apparatus for 10 min. On day 2, mice underwent a training phase followed by a testing phase. During the training phase, mice were placed in the apparatus containing two identical objects positioned in fixed locations and were allowed to freely explore for 5 min. After training, mice were returned to their home cages for a 1-h retention interval.

For the testing phase, mice were reintroduced into the same apparatus for 5 min. One of the two objects remained in its original location (familiar object location, FOL), whereas the other object was moved to a novel location within the arena (novel object location, NOL). Object identity remained unchanged between training and testing. Exploration behavior was recorded, and exploration time for each object was quantified. The discrimination index (DI) was calculated using the following formula: (Pérez-García et al., 2016):

$$\text{Time (NOL)-Time (FOL)} \,/\, \text{Time (NOL)+Time (FOL)}$$

A positive DI value indicates a preference for the object in the novel location, a negative value indicates a preference for the familiar location, and a value of zero indicates equal exploration of both locations.

Chemogenetic manipulation

To enable chemogenetic manipulation of CCK-expressing neurons, CCK-Cre mice were bilaterally implanted with guide cannulas targeting the CA1 region of the hippocampus following viral injection. Stereotaxic coordinates relative to bregma were as follows: anteroposterior (AP), −1.75 mm; mediolateral (ML), ± 1.25 mm; dorsoventral (DV), −1.20 mm. The surgical procedures for cannula implantation were identical to those described above.

Four weeks after viral injection, mice underwent hippocampal-dependent behavioral testing, including the Morris water maze (MWM) and novel object location (NOL) tasks, as well as electrophysiological recordings. Prior to behavioral testing, mice expressing the inhibitory

DREADD hM4D(Gi) and control mice expressing mCherry received bilateral microinfusions of clozapine-N-oxide (CNO; 10 μM in 0.1% DMSO) into the CA1 region. For each infusion, 300 nL of CNO solution was delivered per side at a rate of 50 nL/min using a programmable microinjector.

For in vitro electrophysiological experiments, CNO (50 μM) was bath-applied by adding it to the perfusing artificial cerebrospinal fluid (aCSF) during field excitatory postsynaptic potential (fEPSP) recording sessions.

Fiber photometry recording

Fiber photometry recordings were performed using a commercially available system (Doric Lenses). Sinusoidally modulated light-emitting diodes (LEDs) at 473 nm (220 Hz) and 405 nm (330 Hz) were used to excite the calcium-dependent GCaMP fluorescence signal and the calcium-independent isosbestic control signal, respectively. Excitation light was delivered through an implanted optical fiber, with the output power calibrated to 10 μW at the fiber tip. Fluorescence emission was collected through the same optical fiber and directed to two independent photoreceivers (Model 2151, Newport Corporation). LED modulation, signal acquisition, and real-time demodulation of the 473 nm and 405 nm fluorescence signals were controlled by an RZ5P data acquisition system equipped with a real-time processor (Tucker-Davis Technologies). During behavioral experiments, object exploration in the novel object location (NOL) task was defined as the mouse approaching, sniffing, or touching an object. To enable concurrent fiber photometry recordings, a simplified version of the Morris water maze (MWM) task was used, as previously described (Qin et al., 2018). All photometry data were analyzed using the open-source pMAT software package (Bruno et al., 2021). The raw 473 nm GCaMP signal was corrected for motion-related artifacts by fitting the 405 nm isosbestic signal to the 473 nm channel. The normalized calcium signal was expressed as ΔF/F and calculated using the following formula: ΔF/F = (473 nm signal - fitted 405 nm signal) / fitted 405 nm signal.

Anatomy and histology

All animals were anesthetized with sodium pentobarbital and were perfused with phosphate-buffered saline and fixed with paraformaldehyde solution. Then, mouse's brain was detached and submerged into 4 % PFA solution for fixations at 4 °C in the refrigerator. The brains were sectioned into 40 mm-thick slices via the vibratome machine. The prepared brain sections were counter-stained with DAPI (1:10000) and mounted onto grass slides with 70% glycerol in PBS to observe the AAV expression and fiber track. Finally, the coverslips were used to cover the brain slices and sealed with adhesive glue.

For the histological procedure, brain slices were washed with 0.01 M PBS and blocked with blocking solution (15 % goat serum mixed with 0.4 % Triton X-100) at room temperature for 2-3 h. Then, the primary antibody was prepared and incubated with brain slices in 24-well cell culture plates overnight at 4 °C. Then, brain slices were washed by 0.01 M PBS and coupled to a secondary antibody at room temperature for 2-3 h. Next, brain slices were washed with PBS and were stained with DAPI. Finally, fluorescence image of brain slices was captured by using a Nikon Eclipse fluorescence microscope and a Nikon A1HD25 confocal microscope.

Statistical analysis

All statistical analyses (including two sample t-test, and two-way mixed ANOVA) were done in SPSS (IBM, USA). Statistical significance was set at $p < 0.05$.

Supplementary Figures

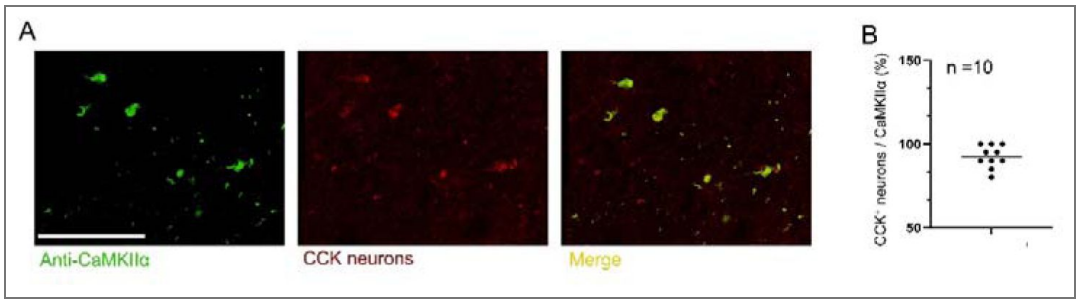

sFigure1. Excitatory CA3 neurons secret the neuropeptide CCK. (A) Representative fluorescent images show that colocalization of the CaMKIIα and CCK^+ neurons. Scale bar = 50 μm. **(B)** Quantitative analysis shows the ratio between CCK^+ neurons and CaMKIIα in the CA3 area.

sFigure2. CA3^{CCK} neurons fire actively during hippocampal-dependent tasks.

(A) Representative fluorescence images showing colocalization of CCK-positive neurons with the excitatory neuronal marker CaMKIIα in the CA3 region. Scale bar = 50 μm. **(B)** Quantification of the proportion of CCK-positive neurons that co-express CaMKIIα in the CA3 area.

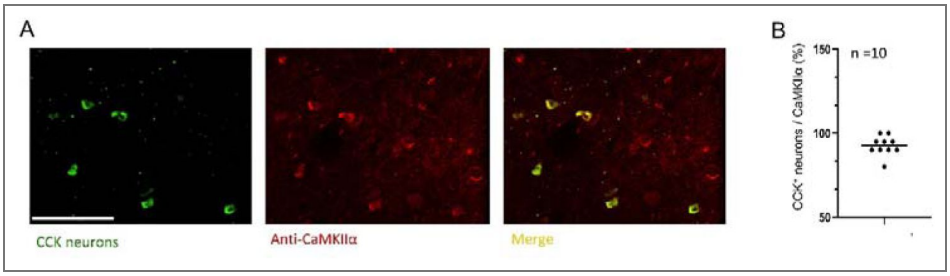

sFigure3. Chemogenetic inhibition of the excitatory CA3^{CCK}-CA1 pathway impairs behavioral tasks.

(A) Representative fluorescent images show that colocalization of the CaMKIIα and CCK neurons. Scale bar = 50 μm. **(B)** Quantitative analysis shows the ratio between CCK neurons and CaMKIIα in the CA3 area.

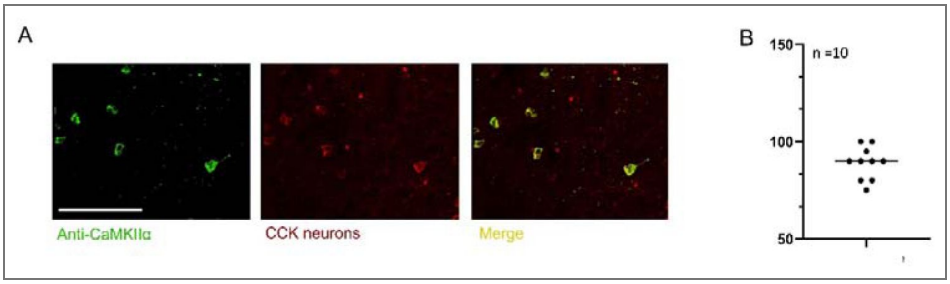

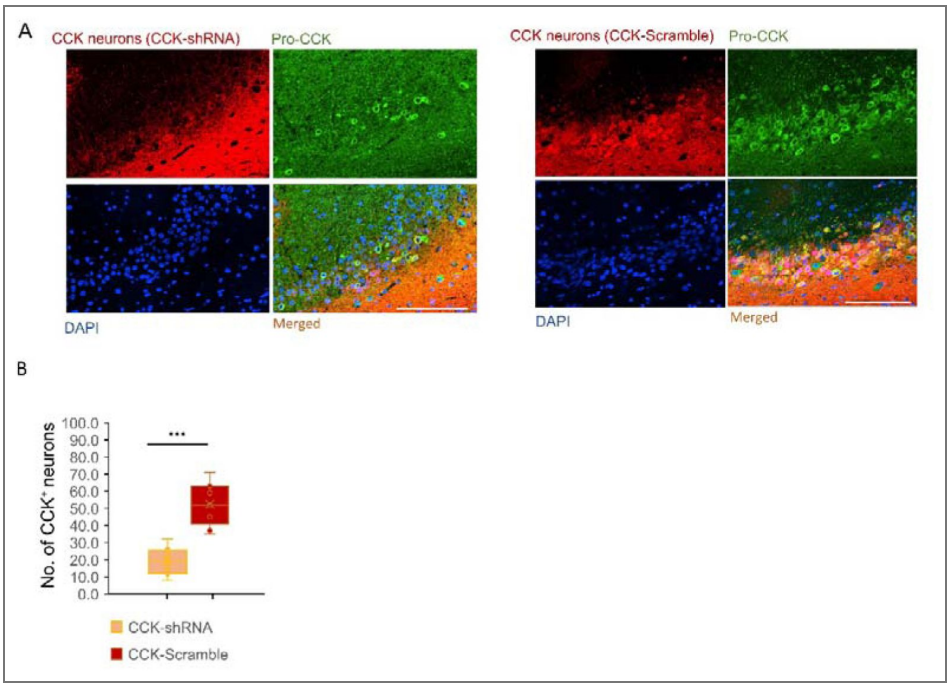

sFigure4. RNA interference of excitatory CA3^{CCK}expression attenuates hippocampal functions.

(A) Representative fluorescent images show that CCK-shRNA (left panel) significantly reduced CCK expression in CA3 -positive neurons compared with the CCK-Scramble group (right panel). Scale bar = 50 μm. **(B)** Quantitative analysis shows the number of CCK neurons, defined by colocalization of CCK and Pro-CCK, in the CCK-shRNA and CCK-Scramble groups (n = 9 slices for each group). ∗p < 0.05, ∗∗p < 0.01, ∗∗∗p < 0.001; ns, not significant. Data are reported as mean ± SEM.

Data availability

The data that support the findings of this study are available from the corresponding author upon reasonable request

Acknowledgements

We thank Prof. Jufang He for providing resources. This work was supported by funding from the following: Hong Kong Research Grants Council, General Research Fund: CityUHK 11101521, CityUHK 11103922, CityUHK 11104923, CityUHK 11104524.

Additional information

Author contributions

Conceptualization: H.F; Methodology: H.F; Investigation: H.F and A.B; Writing: H.F. and S.T.B.

Author ORCID iDs

Fengwen Huang: https://orcid.org/0000-0002-3188-6559

References

Ali Afia B (2007) Presynaptic Inhibition of $GABA_A$ Receptor-Mediated Unitary IPSPs by Cannabinoid Receptors at Synapses Between CCK-Positive Interneurons in Rat Hippocampus. *Journal of Neurophysiology* **98**:861-69 https://doi.org/10.1152/jn.00156.2007 | PubMed

Birthelmer A, et al. (2003) Neurotransmitter Release and Its Presynaptic Modulation in the Rat Hippocampus after Selective Damage to Cholinergic or/and Serotonergic Afferents. *Brain Research Bulletin* **59**:371-81 https://doi.org/10.1016/s0361-9230(02)00930-9 | PubMed

Böhme Georg Andrees, Stutzmann Jean-Marie, Blanchard Jean-Charles (1988) Excitatory Effects of Cholecystokinin in Rat Hippocampus: Pharmacological Response Compatible with 'Central'- or B-Type CCK Receptors. *Brain Research* **451**:309-18 https://doi.org/10.1016/0006-8993(88)90776-7 | PubMed

Broussard John I., et al. (2016) Dopamine Regulates Aversive Contextual Learning and Associated In Vivo Synaptic Plasticity in the Hippocampus. *Cell Reports* **14**:1930-39 https://doi.org/10.1016/j.celrep.2016.01.070 | PubMed

Bruno Carissa A., et al. (2021) pMAT: An Open-Source Software Suite for the Analysis of Fiber Photometry Data. *Pharmacology Biochemistry and Behavior* **201**:173093 https://doi.org/10.1016/j.pbb.2020.173093 | PubMed

Cai Xiang, et al. (2013) Local Potentiation of Excitatory Synapses by Serotonin and Its Alteration in Rodent Models of Depression. *Nature Neuroscience* **16**:464-72 https://doi.org/10.1038/nn.3355 | PubMed

Cai Yuan, Ford Christopher P. (2018) Dopamine Cells Differentially Regulate Striatal Cholinergic Transmission across Regions through Corelease of Dopamine and Glutamate. *Cell Reports* **25**:3148-3157. https://doi.org/10.1016/j.celrep.2018.11.053 | PubMed

Chang Chin-Chyuan, Hung Ming-Di, Cheng Winton (2011) Norepinephrine Depresses the Immunity and Disease-Resistance Ability via A1- and B1-Adrenergic Receptors of Macrobrachium Rosenbergii. *Developmental & Comparative Immunology* **35**:685-91 https://doi.org/10.1016/j.dci.2011.01.020 | PubMed

Chen Lei, et al. (2021) Cholecystokinin Octapeptide Improves Hippocampal Glutamatergic Synaptogenesis and Postoperative Cognition by Inhibiting Induction of A1 Reactive Astrocytes in Aged Mice. *CNS Neuroscience & Therapeutics* **27**:1374-84 https://doi.org/10.1111/cns.13718 | PubMed

Chowdhury Rumana, et al. (2012) Dopamine Modulates Episodic Memory Persistence in Old Age. *The Journal of Neuroscience* **32**:14193-204 https://doi.org/10.1523/jneurosci.1278-12.2012 | PubMed

De Wied D (1997) Neuropeptides in Learning and Memory Processes. *Behavioural Brain Research* **83**:83-90

Ge Yuan, et al. (2010) Hippocampal Long-Term Depression Is Required for the Consolidation of Spatial Memory. *Proceedings of the National Academy of Sciences* **107**:16697-702 https://doi.org/10.1073/pnas.1008200107 | PubMed

Gedankien Tamara, et al. (2023) Acetylcholine Modulates the Temporal Dynamics of Human Theta Oscillations during Memory. *Nature Communications* **14**:5283 https://doi.org/10.1038/s41467-023-41025-y | PubMed

Gomez Juan L., et al. (2017) Chemogenetics Revealed: DREADD Occupancy and Activation via Converted Clozapine. *Science* **357**:503-7 https://doi.org/10.1126/science.aan2475 | PubMed

Goodman Anthoni M., et al. (2021) Heightened Hippocampal β-Adrenergic Receptor Function Drives Synaptic Potentiation and Supports Learning and Memory in the TgF344-AD Rat Model during Prodromal Alzheimer's Disease. *The Journal of Neuroscience* **41**:5747-61 https://doi.org/10.1523/jneurosci.0119-21.2021 | PubMed

Grasselli Giorgio, Hansel Christian (2014) Cerebellar Long-Term Potentiation. In: Mauk MD (Ed). *International Review of Neurobiology* Elsevier. pp. 39-51 https://doi.org/10.1016/b978-0-12-420247-4.00003-8 | PubMed

Hamilton Trevor J., et al. (2010) Dopamine Modulates Synaptic Plasticity in Dendrites of Rat and Human Dentate Granule Cells. *Proceedings of the National Academy of Sciences* **107**:18185-90 https://doi.org/10.1073/pnas.1011558107 | PubMed

Hartzell Andrea L, et al. (2018) NPAS4 Recruits CCK Basket Cell Synapses and Enhances Cannabinoid-Sensitive Inhibition in the Mouse Hippocampus. *eLife* **7**:e35927 https://doi.org/10.7554/eLife.35927 | PubMed

Hefft Stefan, Jonas Peter (2005) Asynchronous GABA Release Generates Long-Lasting Inhibition at a Hippocampal Interneuron-Principal Neuron Synapse. *Nature Neuroscience* **8**:1319-28 https://doi.org/10.1038/nn1542 | PubMed

Karayol Remzi, et al. (2021) Serotonin Receptor 4 in the Hippocampus Modulates Mood and Anxiety. *Molecular Psychiatry* **26**:2334-49 https://doi.org/10.1038/s41380-020-00994-y | PubMed

Kempadoo Kimberly A., et al. (2016) Dopamine Release from the Locus Coeruleus to the Dorsal Hippocampus Promotes Spatial Learning and Memory. *Proceedings of the National Academy of Sciences* **113**:14835-40 https://doi.org/10.1073/pnas.1616515114 | PubMed

Klausberger Thomas, et al. (2005) Complementary Roles of Cholecystokinin- and Parvalbumin-Expressing GABAergic Neurons in Hippocampal Network Oscillations. *The Journal of Neuroscience* **25**:9782-93 https://doi.org/10.1523/jneurosci.3269-05.2005 | PubMed

Lopes L.V., et al. (2002) Adenosine A2A Receptor Facilitation of Hippocampal Synaptic Transmission Is Dependent on Tonic A1 Receptor Inhibition. *Neuroscience* **112**:319-29 https://doi.org/10.1016/s0306-4522(02)00080-5 | PubMed

Ma Yihe, Giardino William J. (2022) Neural Circuit Mechanisms of the Cholecystokinin (CCK) Neuropeptide System in Addiction. *Addiction Neuroscience* **3**:100024 https://doi.org/10.1016/j.addicn.2022.100024 | PubMed

Martin S. J., Clark R. E. (2007) The Rodent Hippocampus and Spatial Memory: From Synapses to Systems. *Cellular and Molecular Life Sciences* **64**:401-31 https://doi.org/10.1007/s00018-007-6336-3 | PubMed

Merighi Adalberto, Salio Chiara, Ferrini Francesco, Lossi Laura (2011) Neuromodulatory Function of Neuropeptides in the Normal CNS. *Journal of Chemical Neuroanatomy* **42**:276-87 https://doi.org/10.1016/j.jchemneu.2011.02.001 | PubMed

Mineur Yann S., et al. (2013) Cholinergic Signaling in the Hippocampus Regulates Social Stress Resilience and Anxiety- and Depression-like Behavior. *Proceedings of the National Academy of Sciences* **110**:3573-78 https://doi.org/10.1073/pnas.1219731110 | PubMed

Mlinar Boris, Stocca Gabriella, Corradetti Renato (2015) Endogenous Serotonin Facilitates Hippocampal Long-Term Potentiation at CA3/CA1 Synapses. *Journal of Neural Transmission* **122**:177-85 https://doi.org/10.1007/s00702-014-1246-7 | PubMed

Mohajerani Majid H., et al. (2007) Correlated Network Activity Enhances Synaptic Efficacy via BDNF and the ERK Pathway at Immature CA3-CA1 Connections in the Hippocampus. *Proceedings of the National Academy of Sciences* **104**:13176-81 https://doi.org/10.1073/pnas.0704533104 | PubMed

Nakamura N.H., Akiyama K., Naito T. (2011) Suppression of cAMP-Dependent Gene Expression by Cholecystokinin in the Hippocampus. *Neuroscience* **187**:15-23 https://doi.org/10.1016/j.neuroscience.2011.04.031 | PubMed

Nishimura Sayoko, et al. (2015) Functional Synergy between Cholecystokinin Receptors CCKAR and CCKBR in Mammalian Brain Development. *PLOS One* **10**:e0124295 https://doi.org/10.1371/journal.pone.0124295 | PubMed

Ohta Kohei, et al. (2003) Stearic Acid Facilitates Hippocampal Neurotransmission by Enhancing Nicotinic ACh Receptor Responses via a PKC Pathway. *Molecular Brain Research* **119**:83-89 https://doi.org/10.1016/j.molbrainres.2003.08.017 | PubMed

Park Hyungju, Popescu Andrei, Poo Mu-ming (2014) Essential Role of Presynaptic NMDA Receptors in Activity-Dependent BDNF Secretion and Corticostriatal LTP. *Neuron* **84**:1009-22 https://doi.org/10.1016/j.neuron.2014.10.045 | PubMed

Pérez-García Georgina, Guzmán-Quevedo Omar, Da Silva Aragão Raquel, Bolaños-Jiménez Francisco (2016) Early Malnutrition Results in Long-Lasting Impairments in Pattern-Separation for Overlapping Novel Object and Novel Location Memories and Reduced Hippocampal Neurogenesis. *Scientific Reports* **6**:21275 https://doi.org/10.1038/srep21275 | PubMed

Picciotto Marina R., Higley Michael J., Mineur Yann S. (2012) Acetylcholine as a Neuromodulator: Cholinergic Signaling Shapes Nervous System Function and Behavior. *Neuron* **76**:116-29 https://doi.org/10.1016/j.neuron.2012.08.036 | PubMed

Qin Han, et al. (2018) A Visual-Cue-Dependent Memory Circuit for Place Navigation. *Neuron* **99**:47-55.e4 https://doi.org/10.1016/j.neuron.2018.05.021 | PubMed

Ranganath Charan, Hsieh Liang-Tien (2016) The Hippocampus: A Special Place for Time: The Hippocampus: A Special Place for Time. *Annals of the New York Academy of Sciences* **1369**:93-110 https://doi.org/10.1111/nyas.13043 | PubMed

Reisi Parham, et al. (2015) Effect of Cholecystokinin on Learning and Memory, Neuronal Proliferation and Apoptosis in the Rat Hippocampus. *Advanced Biomedical Research* **4**:227 https://doi.org/10.4103/2277-9175.166650 | PubMed

Swaab D.F (1982) Neuropeptides. Their Distribution and Function in the Brain. In: Buijs R.M., Pévet P., Swaab D.F (Eds). *Progress in Brain Research* Elsevier. pp. 97-122 https://doi.org/10.1016/s0079-6123(08)64192-8 | PubMed

Su J., Huang F., Tian Y., Tian R., Qianqian G., Bello S. T., ..., He J (2023) Entorhinohippocampal cholecystokinin modulates spatial learning by facilitating neuroplasticity of hippocampal CA3-CA1 synapses. *Cell Reports* **42** https://doi.org/10.1016/j.celrep.2023.113467 | PubMed

Takács Virág T., et al. (2018) Co-Transmission of Acetylcholine and GABA Regulates Hippocampal States. *Nature Communications* **9**:2848 https://doi.org/10.1038/s41467-018-05136-1 | PubMed

Vorhees Charles V, Williams Michael T (2006) Morris Water Maze: Procedures for Assessing Spatial and Related Forms of Learning and Memory. *Nature Protocols* **1**:848-58 https://doi.org/10.1038/nprot.2006.116 | PubMed

Wei Xiao-fei, et al. (2013) CCK-8S Increases the Firing Frequency of CCK-Positive Neurons and Facilitates Excitatory Synaptic Transmission in Primary Rat Hippocampal Neurons. *Neuroscience Letters* **549**:34-39 https://doi.org/10.1016/j.neulet.2013.06.043 | PubMed

Wen Di, et al. (2014) Cholecystokinin-Octapeptide Restored Morphine-Induced Hippocampal Long-Term Potentiation Impairment in Rats. *Neuroscience Letters* **559**:76-81 https://doi.org/10.1016/j.neulet.2013.11.043 | PubMed

Whissell Paul D., et al. (2019) Selective Activation of Cholecystokinin-Expressing GABA (CCK-GABA) Neurons Enhances Memory and Cognition. *eneuro* **6**:ENEURO.0360-18.2019 https://doi.org/10.1523/eneuro.0360-18.2019 | PubMed

Xing Bo, Li Yan-Chun, Gao Wen-Jun (2016) Norepinephrine versus Dopamine and Their Interaction in Modulating Synaptic Function in the Prefrontal Cortex. *Brain Research* **1641**:217-33 https://doi.org/10.1016/j.brainres.2016.01.005 | PubMed

Zakharenko Stanislav S, et al. (2003) Presynaptic BDNF Required for a Presynaptic but Not Postsynaptic Component of LTP at Hippocampal CA1-CA3 Synapses. *Neuron* **39**:975-90 https://doi.org/10.1016/s0896-6273(03)00543-9 | PubMed

Zhang N., Sui Y., Jendrichovsky P., Feng H., Shi H., Zhang X., ..., He J. (2024) Cholecystokinin B receptor agonists alleviates anterograde amnesia in cholecystokinin-deficient and aged Alzheimer's disease mice. *Alzheimer's research & therapy* **16**:109 https://doi.org/10.1186/s13195-024-01472-1 | PubMed

Peer reviews

Reviewer #1 (Public review):

Summary:

CCK is the most abundant neuropeptide in the brain, and many studies have investigated the role of CCK and inhibitory CCK interneurons in modulating neural circuits, especially in the hippocampus. The manuscript presents interesting questions regarding the role of excitatory CCK+ neurons in the hippocampus, which has been much less studied compared to the well-known roles of inhibitory CCK neurons in regulating network function. The authors adopt several methods including transgenic mice and viruses, optogenetics, chemogenetics, RNAi, and behavioral tasks to explore these less-studied roles of excitatory CCK neurons in CA3. They find that the excitatory CCK neurons are involved in hippocampal-dependent tasks such as spatial learning and memory formation, and that CCK-knockdown impairs these tasks.

However, these questions are very dependent on ensuring that the study is properly targeting excitatory CCK neurons (and thus their specific contributions to behavior).

There needs to be much more characterization of the CCK transgenic mice and viruses to confirm the targeting. Without this, it is unclear whether the study is looking at excitatory CCK neurons or a more general heterogeneous CCK neuron population.

Strengths:

This field has focused mainly on inhibitory CCK+ interneurons and their role in network function and activity, and thus this manuscript raises interesting questions regarding the role of excitatory CCK+ neurons, which have been much less studied.

Weaknesses:

(1a) This manuscript is dependent on ensuring that the study is indeed investigating the role of excitatory CCK-expressing neurons themselves and their specific contribution to behavior. There needs to be much more characterization of the CCK-expressing mice (crossed with Ai14 or transduced with various viruses) to confirm the excitatory-cell targeting. Without this, it is

unclear whether the study is looking at excitatory CCK neurons or a more general heterogeneous CCK neuron population.

(2) The methods and figure legends are still extremely sparse, still leading to many questions regarding methodology and accuracy. More details would be useful in evaluating the tools and data, and the lack of proper quantification is still prevalent throughout the paper. In many places, only % values are noted, or only images are presented, and the number of cells counted is almost never reported.

https://doi.org/10.7554/eLife.109001.2.sa3

Reviewer #2 (Public review):

Summary:

In this study, the authors have demonstrated, through a comprehensive approach combining electrophysiology, chemogenetics, fiber photometry, RNA interference, and multiple behavioral tasks, the necessity of projections from CCK+ CAMKIIergic neurons in the hippocampal CA3 region to the CA1 region for regulating spatial memory in mice. Specifically, authors have shown that CA3-CCK CAMKIIergic neurons are selectively activated by novel locations during a spatial memory task. Furthermore, authors have identified the CA3-CA1 pathway as crucial for this spatial working memory function, thereby suggesting a pivotal role for CA3 excitatory CCK neurons in influencing CA1 LTP. The data presented appear to be well-organized and comprehensive.

Strengths:

(1) This work combined various methods to validate the excitatory CCK neurons in the CA3 area; these data are convincing and solid.

(2) This study demonstrated that the CA3-CCK CAMKIIergic neurons are involved in the spatial memory tasks; these are interesting findings, which suggest that these neurons are important targets for manipulating the memory-related diseases.

(3) This manuscript also measured the endogenous CCK from the CA3-CCK CAMKIIergic neurons; this means that CCK can be released under certain conditions.

Weaknesses:

In summary, this work can be formally accepted after the revision. For the limitations of the revision, the distinct neural effects of cholecystokinin (CCK) receptors (CCK-1R, CCK-2R, and CCK-3R) on hippocampal function have not been fully elucidated. Recent studies indicate that CCK-2R can modulate hippocampal activity at CA3-Schaffer collateral synapses; however, the roles of CCK-1R and CCK-3R in hippocampal function remain poorly characterized, with limited experimental evidence supporting their involvement. Overall, this study provides an interesting and novel perspective on the role of excitatory CCK signaling in hippocampus-dependent navigation learning.

https://doi.org/10.7554/eLife.109001.2.sa2

Reviewer #3 (Public review):

Summary:

Fengwen Huang et al. used multiple neuroscience techniques (transgenetic mouse, immunochemistry, bulk calcium recording, neural sensor, hippocampal-dependent task, optogenetics, chemogenetics, and interfer RNA technique) to elucidate the role of the

excitatory cholecystokinin-positive pyramidal neurons in the hippocampus in regulating the hippocampal functions, including navigation and neuroplasticity.

Strengths:

(i) The authors provided the distribution profiles of excitatory cholecystokinin in the dorsal hippocampus via the transgenetic mice (Ai14::CCK Cre mice), immunochemistry, and retrograde AAV.

(ii) The authors used the neural sensor and light stimulation to monitor the CCK release from the CA3 area, indicating that CCK can be secreted by activation of the excitatory CCK neurons.

(iii) The authors showed that the activity of the excitatory CCK neurons in CA3 is necessary for navigation learning

(iv) The authors demonstrated that inhibition of the excitatory CCK neurons and knockdown of the CCK gene expression in CA3 impaired the navigation learning and the neuroplasticity of CA3-CA1 projections.

Weaknesses:

(i) The causal relationship between navigation learning and CCK secretion remains nebulous; answering this question will require a more sensitive CCK-BR sensor in future work.

https://doi.org/10.7554/eLife.109001.2.sa1

Author response:

The following is the authors' response to the original reviews.

> ***Public Reviews:***
>
> ***Reviewer #1 (Public review):***
>
> *Summary:*
>
> *CCK is the most abundant neuropeptide in the brain, and many studies have investigated the role of CCK and inhibitory CCK interneurons in modulating neural circuits, especially in the hippocampus. The manuscript presents interesting questions regarding the role of excitatory CCK+ neurons in the hippocampus, which has been much less studied compared to the well-known roles of inhibitory CCK neurons in regulating network function. The authors adopt several methods, including transgenic mice and viruses, optogenetics, chemogenetics, RNAi, and behavioral tasks to explore these less-studied roles of excitatory CCK neurons in CA3. They find that the excitatory CCK neurons are involved in hippocampal-dependent tasks such as spatial learning and memory formation, and that CCK-knockdown impairs these tasks.*
>
> *However, these questions are very dependent on ensuring that the study is properly targeting excitatory CCK neurons (and thus their specific contributions to behavior). There needs to be much more characterization of the CCK transgenic mice and viruses to confirm the targeting. Without this, it is unclear whether the study is looking at excitatory CCK neurons or a more general heterogeneous CCK neuron population.*
>
> *Strengths:*
>
> *This field has focused mainly on inhibitory CCK+ interneurons and their role in network function and activity, and thus, this manuscript raises interesting questions regarding the role of excitatory CCK+ neurons, which have been much less studied.*

> *Weaknesses:*
>
> *(1a) This manuscript is dependent on ensuring that the study is indeed investigating the role of excitatory CCK-expressing neurons themselves and their specific contribution to behavior. There needs to be much more characterization of the CCK-expressing mice (crossed with Ai14 or transduced with various viruses) to confirm the excitatory-cell targeting. Without this, it is unclear whether the study is looking at excitatory CCK neurons or a more general heterogeneous CCK neuron population.*

Thank you for this constructive comment. Indeed, the current study lacks comprehensive strategies to unequivocally distinguish excitatory CCK neurons from heterogeneous CCK neuronal populations. Nevertheless, we provide multiple lines of evidence supporting the distribution of CaMKIIα/Vglut1-expressing CCK^+ neurons in the hippocampus (Figure 1F), using complementary approaches including transgenic mouse models as well as viral and antibody-based labeling (Figure 1A, Figure 1H-I). In addition, we demonstrate that 635 nm light reliably evokes field excitatory postsynaptic potentials (fEPSPs) at CA3-Schaffer collateral synapses expressing DIO-CaMKIIα-ChrimsonR *in vitro* (Figure 2A-F). Importantly, these light-evoked excitatory synaptic responses are abolished by AMPA and NMDA receptor antagonists (CNQX and APV), confirming the excitatory nature of the DIO-CaMKIIα-ChrimsonR-expressing synapses. To demonstrate the future works that can further support our findings and conclusions, we have added the strategies that can be conducted in the Discussion section in the revision:

"Due to technical limitations at the current stage, we were unable to perform whole-cell recordings or pharmacological manipulations using CCK receptor antagonists. In future studies, the application of these approaches to directly record and selectively block EPSPs from excitatory CCK neurons in the hippocampus will further strengthen and validate our conclusions." (Line 265 - line 269 in the revision).

> *(1b) For the experiments that use a virus with the CCK-IRES-Cre mouse, there is no information or characterization on how well the virus targets excitatory CCK-expressing neurons. (Additionally, it has been reported that with CaMKIIa-driven protein expression, using viruses, can be seen in both pyramidal and inhibitory cells.*

We thank the reviewer for this insightful comment regarding the specificity of viral targeting in CCK-IRES-Cre mice.

To address this concern, we performed additional characterization of viral expression in CA3. We found that DIO-CaMKIIα-mCherry expression showed a high degree of colocalization with CaMKIIα immunoreactivity, indicating preferential targeting of excitatory neurons (sFigure 1A-B; sFigure 2A-B; sFigure 3A-B). We showed an example to confirmed the high specificity of the AAV for infecting the excitatory CCK neurons in CA3 area.

Besides, we acknowledge prior reports showing that CaMKIIα-driven viral expression can, in some cases, be detected in a small subset of inhibitory neurons. However, because CA3-Schaffer collateral projections to CA1 arise exclusively from excitatory CA3 pyramidal neurons, any potential expression in inhibitory CCK^+ interneurons are unlikely to directly contribute to the recorded CA1 synaptic responses in our electrophysiological experiments. That said, we cannot fully exclude the possibility that a minor population of inhibitory CCK^+ neurons could indirectly modulate CA3 pyramidal neuron activity via local circuit mechanisms, particularly in experiments involving optogenetic manipulation or shRNA expression. We now explicitly acknowledge this limitation in the revised manuscript:

"Importantly, to further improve cell-type specificity, we propose an intersectional genetic strategy using CCK-IRES-Cre × VGlut1-Flp mice combined with a Cre-On/Flp-On (Con/Fon) AAV, which would restrict expression exclusively to excitatory CCK-expressing neurons and

eliminate potential contributions from inhibitory CCK^+ cells. This approach will be implemented in future studies to refine circuit specificity." (Line 269 - line 273 in the revision).

> *(2) The methods and figure legends are extremely sparse, leading to many questions regarding methodology and accuracy. More details would be useful in evaluating the tools and data. More details would be useful in evaluating the tools and data. Additionally, further quantification would be useful-e.g. in some places, only % values are noted, or only images are presented.*

Thank you for these constructive comments. We have expanded the methodological descriptions in both the Methods section and the figure legends to provide sufficient detail for evaluating the experimental tools and data accuracy. In addition, we have added quantitative analyses where previously only representative images or percentage values were shown. Specifically, quantification has now been included for each AAV condition in the corresponding figures in the revised manuscript.

> *(3) It is unclear whether the reduced CCK expression is correlated, or directly causing the impairments in hippocampal function. Does the CCK-shRNA have any additional detrimental effects besides affecting CCK-expression (e.g., is the CCK-shRNA also affecting some other essential (but not CCK-related) aspect of the neuron itself?)? Is there any histology comparison between the shRNA and the scrambled shRNA?*

Recent studies from our lab demonstrated that knockout the CCK gene expression significantly attenuates the hippocampal-dependent spatial learning and CA3-CA1 LTP, indicating CCK plays a critical role in modulating the hippocampal functions[1,2]. Additionally, CCK-shRNA or CCK-scramble did not significantly affect the excitatory synaptic transmission in the CA3-CA1 projections, hinting that CCK-shRNA may exhibits no obvious adverse effect on other neural components.

Finally, we have provided the histology comparison between the shRNA and the scrambled shRNA regrading the expression level of the CCK protein (Pro-CCK) in the revision. Our result shows that CCK-shRNA (left panel) significantly reduced CCK expression in $CA3^{CCK}$-positive neurons compared with the CCK-Scramble group (right panel).

Citation:

(1) Wang, J. L., Sha, X. Y., Shao, Y., Zhang, Z. H., Huang, S. M., Lin, H., ... & Sun, J. P. (2025). Elucidating pathway-selective biased CCKBR agonism for Alzheimer's disease treatment. Cell.

(2) Zhang, N., Sui, Y., Jendrichovsky, P., Feng, H., Shi, H., Zhang, X., ... & He, J. (2024). Cholecystokinin B receptor agonists alleviates anterograde amnesia in cholecystokinin-deficient and aged Alzheimer's disease mice. Alzheimer's research & therapy, 16(1), 109.

https://doi.org/10.7554/eLife.109001.1.sa2

> ***Reviewer #2 (Public review):***
>
> *Summary:*
>
> *In this study, the authors have demonstrated, through a comprehensive approach combining electrophysiology, chemogenetics, fiber photometry, RNA interference, and multiple behavioral tasks, the necessity of projections from CCK+ CAMKIIergic neurons in the hippocampal CA3 region to the CA1 region for regulating spatial memory in mice. Specifically, authors have shown that CA3-CCK CAMKIIergic neurons are selectively activated by novel locations during a spatial memory task. Furthermore, authors have identified the CA3-CA1 pathway as crucial for this spatial working memory function,*

> *thereby suggesting a pivotal role for CA3 excitatory CCK neurons in influencing CA1 LTP. The data presented appear to be well-organized and comprehensive.*
>
> *Strengths:*
>
> *(1) This work combined various methods to validate the excitatory CCK neurons in the CA3 area; these data are convincing and solid.*
>
> *(2) This study demonstrated that the CA3-CCK CAMKIIergic neurons are involved in the spatial memory tasks; these are interesting findings, which suggest that these neurons are important targets for manipulating the memory-related diseases.*
>
> *(3) This manuscript also measured the endogenous CCK from the CA3-CCK CAMKIIergic neurons; this means that CCK can be released under certain conditions.*
>
> *Weaknesses:*
>
> *(1) The authors do not mention which receptors of the CCK modulate these processes.*

We appreciate the reviewer for raising this important question. Based on our recent work, CCK-B receptors are the primary neural components mediating CCK functions in the hippocampus at both the synaptic plasticity and behavioral levels (Su et al., 2023; Zhang et al., 2024; Wang et al., 2025). To clarify this mechanism, we have added the following content to the revised manuscript:

"Based on our recent work, CCK signaling in the hippocampus is predominantly mediated by CCK-B receptors, which play a critical role in regulating synaptic plasticity and spatial memory-related behaviors." (Line 105 - line 106 in the revision).

> *(2) This author does not test the CCK gene knockout mice or the CCK receptor knockout mice in these neural processes.*

Thank you for this insightful comment. We previously tested these experiments in an earlier study. Our results showed that high-frequency electrical stimulation failed to induce significant LTP in the CA3-CA1 pathway in both CCK gene knockout (CCK-KO) mice and CCK-B receptor knockout (CCK-BR-KO) mice *in vitro* (Su et al., 2023; Zhang et al., 2024; Wang et al., 2025). These findings indicate that CCK mediates its synaptic effects predominantly through CCK-B receptors in the CA3-CA1 pathway. Accordingly, we have added this description to the revised manuscript.

"Additionally, high-frequency electrical stimulation fails to induce LTP in the CA3-CA1 pathway in both CCK-KO and CCK-BR-KO mice, indicating that CCK-dependent synaptic plasticity in this circuit is primarily mediated by CCK-B receptors." (Line 170 - line 173 in the revision).

> *(3) The author does not test the source of CCK release during the behavioral tasks.*

We thank the reviewer for raising this important point. In our previous work, we directly monitored CCK release in the hippocampus during an object-exploration task using a GPCR-based CCK-BR sensor combined with fiber photometry (Su et al., 2023). During object exploration, we observed a rapid and robust increase in CCK-BR sensor fluorescence, indicating activity-dependent CCK release in the hippocampus. Based on these findings, we deduced that hippocampal CCK release plays a critical role in hippocampus-dependent behavioral tasks.

We acknowledge that hippocampal neurons receive CCK-positive projections from multiple brain regions, making it technically challenging to isolate and monitor the precise source of CCK release in the CA1 area during behavioral tasks *in vivo*. One potential strategy to address

this limitation is selective overexpression of CCK in CA3 neurons (e.g., AAV-CCK delivery), followed by assessment of CCK-BR sensor responses during hippocampal-dependent behaviors. We have added this discussion to the revised manuscript to clarify the source and functional relevance of CCK release during behavioral tasks.

“Besides, using a GPCR-based CCK-BR sensor combined with fiber photometry, our previous work demonstrated rapid, activity-dependent CCK release in the hippocampus during object-exploratory behavior, supporting a functional role for hippocampal CCK signaling in cognitive tasks (Su et al., 2023). Given that hippocampal neurons receive CCK-positive projections from multiple brain regions, it remains technically challenging to precisely identify the cellular source of CCK release in CA1 during behavior. Future studies employing selective CCK overexpression in CA3 neurons, together with CCK-BR sensor recordings, may help further delineate the contribution of CA3-derived CCK to hippocampal-dependent behaviors.” (Line 313 - line 321 in the revision).

Citation:

(1) Wang, J. L., Sha, X. Y., Shao, Y., Zhang, Z. H., Huang, S. M., Lin, H., ... & Sun, J. P. (2025). Elucidating pathway-selective biased CCKBR agonism for Alzheimer’s disease treatment. Cell.

(2) Zhang, N., Sui, Y., Jendrichovsky, P., Feng, H., Shi, H., Zhang, X., ... & He, J. (2024). Cholecystokinin B receptor agonists alleviates anterograde amnesia in cholecystokinin-deficient and aged Alzheimer's disease mice. Alzheimer's research & therapy, 16(1), 109.

(3) Su, J., Huang, F., Tian, Y., Tian, R., Qianqian, G., Bello, S. T., ... & He, J. (2023). Entorhinohippocampal cholecystokinin modulates spatial learning by facilitating neuroplasticity of hippocampal CA3-CA1 synapses. Cell Reports, 42(12).

https://doi.org/10.7554/eLife.109001.1.sa1

Reviewer #3 (Public review):

Summary:

Fengwen Huang et al. used multiple neuroscience techniques (transgenetic mouse, immunochemistry, bulk calcium recording, neural sensor, hippocampal-dependent task, optogenetics, chemogenetics, and interfer RNA technique) to elucidate the role of the excitatory cholecystokinin-positive pyramidal neurons in the hippocampus in regulating the hippocampal functions, including navigation and neuroplasticity.

Strengths:

(1) The authors provided the distribution profiles of excitatory cholecystokinin in the dorsal hippocampus via the transgenetic mice (Ai14::CCK Cre mice), immunochemistry, and retrograde AAV.

(2) The authors used the neural sensor and light stimulation to monitor the CCK release from the CA3 area, indicating that CCK can be secreted by activation of the excitatory CCK neurons.

(3) The authors showed that the activity of the excitatory CCK neurons in CA3 is necessary for navigation learning.

(4) The authors demonstrated that inhibition of the excitatory CCK neurons and knockdown of the CCK gene expression in CA3 impaired the navigation learning and the neuroplasticity of CA3-CA1 projections.

Weaknesses:

> *(1) The causal relationship between navigation learning and CCK secretion?*

Thank you for pointing out this important issue. Previous studies have shown that CCK can be rapidly secreted during exploratory behaviors, as detected by the CCK-BR sensor. In parallel, CCK-positive neurons have been demonstrated to play a critical role in the precise execution of hippocampus-dependent spatial learning. Together, these findings suggest that exploratory behavior induces CCK secretion, which in turn contributes to the accuracy of hippocampal-dependent learning and memory processes. Based on this evidence, we propose that CCK secretion serves as a functional link between behavioral exploration and spatial learning. We have added these explanations in the revised manuscript to better clarify the causal relationship between behavioral exploration and CCK secretion:

"Besides, using a GPCR-based CCK-BR sensor combined with fiber photometry, our previous work demonstrated rapid, activity-dependent CCK release in the hippocampus during object-exploratory behavior, supporting a functional role for hippocampal CCK signaling in cognitive tasks (Su et al., 2023). Given that hippocampal neurons receive CCK-positive projections from multiple brain regions, it remains technically challenging to precisely identify the cellular source of CCK release in CA1 during behavior. Future studies employing selective CCK overexpression in CA3 neurons, together with CCK-BR sensor recordings, may help further delineate the contribution of CA3-derived CCK to hippocampal-dependent behaviors." (Line 313 - line 321 in the revision)

> *(2) The effect of overexpression of the CCK gene on hippocampal functions?*

We thank the reviewer for this comment. In fact, an earlier study from our laboratory demonstrated that intraperitoneal injection of exogenous CCK-4 significantly improved performance in hippocampus-dependent spatial learning tasks in both CCK gene knockout (CCK-KO) mice and Alzheimer's disease (AD) mouse models. These findings suggest that enhancing CCK signaling can ameliorate hippocampal dysfunction at both the behavioral and synaptic plasticity levels (Zhang et al., 2024; Wang et al., 2025). Accordingly, although direct genetic overexpression of CCK in the hippocampus has not yet been extensively characterized, the observed benefits of exogenous CCK delivery support the notion that increased CCK availability positively modulates hippocampal function and spatial learning. We have cited this study in the revised manuscript to support this interpretation.

"Interestingly, an earlier study demonstrated that intraperitoneal injection of exogenous CCK-4 significantly improved performance in hippocampus-dependent spatial learning tasks in both CCK gene knockout (CCK-KO) mice and Alzheimer's disease (AD) mouse models (Zhang et al., 2024). These findings suggest that enhancing CCK signaling can ameliorate hippocampal dysfunction at both the behavioral and synaptic plasticity levels." (Line 291 - line 297 in the revision)

> *(3) What are the functional differences between the excitatory and inhibitory CCK neurons in the hippocampus?*

In the hippocampus, CCK-expressing neurons consist of two major populations with distinct functions: excitatory (glutamatergic) and inhibitory (GABAergic) neurons. Excitatory CCK neurons are relatively sparse and intermingled with pyramidal cells. By releasing glutamate, they directly contribute to excitatory transmission and are thought to participate in synaptic plasticity and information processing related to learning and memory. In contrast, inhibitory CCK neurons are more abundant and include well-characterized interneuron subtypes such as CCK-positive basket cells. These neurons release GABA and primarily target the perisomatic region of pyramidal neurons, providing strong control over neuronal firing. Notably, inhibitory CCK interneurons are highly sensitive to neuromodulatory signals, particularly endocannabinoids via CB1 receptors, enabling dynamic regulation of inhibitory

tone and network activity. Together, excitatory CCK neurons mainly support hippocampal excitation and plasticity, whereas inhibitory CCK neurons regulate network dynamics and spike timing. As the focus of the present study is on excitatory CCK neurons, a detailed comparison between these two populations was not included in the original manuscript.

> *(4) Do CCK sources come from the local CA3 or entorhinal cortex (EC) during the high-frequency electrical stimulation?*

Thank you for this insightful comment. Our data indicate that the CCK detected during high-frequency stimulation originates from CA3 neurons rather than the entorhinal cortex (EC). As shown in Figure 2, we used an optogenetic approach combined with a GPCR-based CCK sensor to selectively examine CCK release from the CA3-CA1 pathway. ChrimsonR was specifically expressed in CA3 neurons projecting to CA1, restricting light stimulation to CA3 axon terminals. In parallel, the CCK sensor was locally expressed in CA1, allowing real-time detection of CCK release at CA3 presynaptic sites. High-frequency light stimulation robustly evoked CCK signals in CA1, demonstrating activity-dependent CCK release from CA3 terminals. Importantly, EC inputs were neither genetically targeted nor optically stimulated in this experiment, excluding the EC as a source of the detected CCK. Together, these results support the conclusion that CCK released during high-frequency stimulation is derived from local CA3 projections to CA1. Similarly, as the focus of the present study is on excitatory CCK neurons in the CA3 area, a detailed comparison between these two CCK sources was not included in the original manuscript.

Citation:

(4) Wang, J. L., Sha, X. Y., Shao, Y., Zhang, Z. H., Huang, S. M., Lin, H., ... & Sun, J. P. (2025). Elucidating pathway-selective biased CCKBR agonism for Alzheimer's disease treatment. Cell.

(5) Zhang, N., Sui, Y., Jendrichovsky, P., Feng, H., Shi, H., Zhang, X., ... & He, J. (2024). Cholecystokinin B receptor agonists alleviates anterograde amnesia in cholecystokinin-deficient and aged Alzheimer's disease mice. Alzheimer's research & therapy, 16(1), 109.

(6) Su, J., Huang, F., Tian, Y., Tian, R., Qianqian, G., Bello, S. T., ... & He, J. (2023). Entorhinohippocampal cholecystokinin modulates spatial learning by facilitating neuroplasticity of hippocampal CA3-CA1 synapses. Cell Reports, 42(12).

https://doi.org/10.7554/eLife.109001.2.sa0